Master's thesis

NTNU
Norwegian University of Science and Technology
Faculty of Medicine
Department of Neuroscience

Andreas Lande

Morphological and physiological characterization of olfactory and multimodal neurons in the lateral horn of the *Heliothinae* moth

Master's thesis in Neuroscience
Supervisor: Professor Bente G. Berg
Trondheim, June 2016

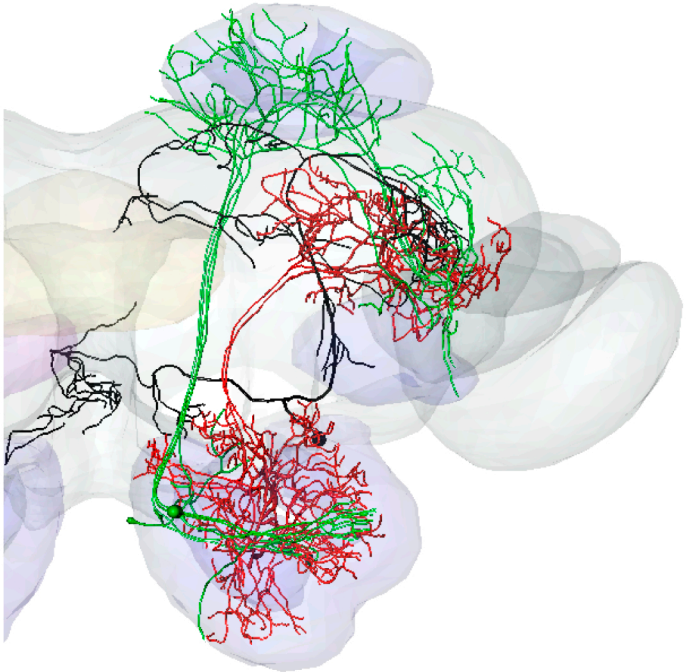

NTNU
Norwegian University of
Science and Technology

* Blank page

On taste and smell, there is no point in arguing.

Hebrew proverb

Acknowledgement

The writing of this thesis has been carried out at the Department of Neuroscience at the Norwegian University of Science and Technology (NTNU), while the experimental work has been completed at the Chemosensory lab, at the Neuroscience Unit of the Department of Psychology.

Humans share an innate drive to explore, to search and to learn. In my search for answers to the most existential questions asked by man, this thesis has been a small part of an educational journey. Several people should receive attention for their motivational influence, helpful insights and caring support.

A special thanks to my mentor and academic advisor for the past year, Professor Bente G. Berg, for her always knowledgeable and interesting inputs. Thanks to Ph.D. candidate Elena Ian, for teaching me the art of electrophysiology and Amira, and for interesting discussions, questions and answers along the way. Thanks to Professor Emeritus Hanna Mustaparta for her ever so deep pond of wisdom and history of the field. Thanks also to my colleague students at the lab, Ida Camilla Kjos and Andreas Panayiotis Goustas.

Finally, I would like to express gratitude to my dear Marie, for her love and laughter, and to my parents for supporting my many years of study.

"Studerende og student. Den er blind som ikke øiner kløften mellom disse to ords betydning. Den som blott er det første uten å være det annet, han blir ingen mann, intet helt menneske - han kan i høiden bare drive det til professor."

Prof. Edgar B. Schieldrop
The first chairman of Samfundet

Trondheim, May 2016

Andreas Lande

Abstract

Through several hundred millions of years, evolution has developed and moulded the chemical senses in animals across our planet, echoing the ever changing environment. In a windy and turbulent field of flowers, insects that try to localize a single flower species embark on a challenging enterprise. Their brain and nervous system have developed key mechanisms to solve such problems. These mechanisms are seen conserved across species, not only limited to insects, but also in fishes and mammals, including humans. To understand how these mechanisms are realized, we must understand the morphological and physiological properties of the olfactory circuits. In this thesis, I have used intracellular recording and iontophoretic staining to investigate neurons in the lateral horn, a higher-order region of the insect brain. This was done *in vivo*, using two related *Heliothinae* moth species as a model organism. The injected fluorescent dye was visualized using confocal laser-scanning microscopy. I show both novel findings on the morphology of antennal-lobe projection neurons, and higher-order neurons innervating the lateral horn, as well as findings that complement previous work. Furthermore, this study shows that neurons in the lateral horn are most responsive to natural odour mixtures, like headspace sample from sunflower and the ideal pheromone mixture emitted by the female of the same species. In addition, I found that 19% of neurons in the lateral horn responding to antennal odour-stimulation also respond to a light stimulus. Finally, a neuronal recording in one female of the species *Helicoverpa armigera* responded to single pheromone components and the ideal mixture, signifying the presence of pheromone autodetection in females of this species.

Table of content

1 | Introduction

Aided by evolution, the nervous system has developed key mechanisms to extract valuable information from the unlabelled environment that surrounds us, by detecting its fundamental properties through our very senses. To further categorize, predict or even manipulate this environment, highly interconnected cellular networks have emerged in the brains of animals. Complex patterns of neuronal spiking activity arise in these networks, serving as a fundamental substrate for information processing (Buzsáki, 2006). Small perturbations in these patterns can cause large effects, as observed in neurological disorders like schizophrenia or epileptic seizures (Fornito et al., 2015). To understand how sensory information is processed by the brain, and how slight deviations in activity result in malfunction, we must understand how the basic sensory mechanisms are realised in a functional nervous system. The insect olfactory system serves as an attractive model system for investigating sensory information processing, as only a few layers of neurons separate input from behavioural output (Ito et al., 2008).

Being one of the evolutionary oldest senses, the sense of smell is found to serve an important role in survival (Nielsen et al., 2015). Throughout the animal kingdom, olfaction plays a vital function in a vast number of aspects of the animal's life, such as mother-child interaction, food-detection, social interaction and detection of predators (Purves, 2012).

Insects are among the most diverse class of animals, estimated to make up almost a million described species (Chapman, 2009). Due to their small size and relatively simple nervous system, many insect species have served as suitable model organisms for studying a functional brain. The holometabolous moth is one insect group contributing to the growing body of knowledge about the olfactory system. One additional reason for studying moths is their destruction of agricultural and horticultural crops such as tomato plants, soy beans, cotton, tobacco and sunflower. The moth species *Heliothis virescens and Helicoverpa armigera*, both used in the present study, are among the major pests on these crops (Fitt, 1989).

1.1 | **Peripheral components of the insect olfactory system**

Due to the vast diversity of insect species, the morphology of their nervous system varies substantially (Strausfeld, 2012). However, we can grossly divide the insect brain into the supraesophageal and subesophageal zone, with the former comprising the deutocerebrum, tritocerebrum and protocerebrum (Ito et al., 2014). For insects, the chemical senses of olfaction and taste, serve as a key part in intra- and interspecific communication. In addition, the chemical senses allow interaction with the environment for detection of host-plants. The olfactory system is able to detect airborne volatile molecules, known as odorants, through an abundance of olfactory receptors (ORs) (Kaupp, 2010). The insect ORs belong to a large family of G protein-coupled receptors, serving as the interface between the external world and the nervous system of the animal (Galizia and Rossler, 2010). These ORs are located on the dendritic end of olfactory sensory neurons (OSNs). While humans and other mammals have the OSNs located in the main olfactory epithelium of the nose, the majority of OSNs in insects are housed in sensilla, hair-shaped protrusions found on the antennas of the insect head (Kaupp, 2010). The number of OSNs found in each sensillum can vary from 2-200 among different species, with 2-4 being typical for moths (Galizia and Rossler, 2010, Lee and Strausfeld, 1990).

While it is generally true for vertebrates that each OSN holds only a single olfactory receptor type, insect OSNs are found to hold two OR types. Together with the common OR, the insect co-receptor Or83b is suggested to form a heterometric complex, creating a non-selective cation ion channel gated directly by relevant plant odor components or pheromone ligands (Sato et al., 2008). It is suggested that such unique receptor-complexes allow us to functionally consider a similar "one OSN – one OR type" rule for insects, comparable to that of vertebrates (Kaupp, 2010). While OSNs housed in the same sensillum do not necessarily share similar ORs, OSNs expressing the same type of OR tend to map to one or two glomeruli in the antennal lobe, the primary center for olfactory information processing (Couto et al., 2005, Galizia and Rossler, 2010). A varying chemical receptive range can be seen among ORs, and their tunings have been typically classified as broad or narrow (Andersson et al., 2015). A broad tuning profile is thought to be allowed through a so called weak-binding, where receptors are activated by a functional group or chemical property of the odorant, in difference to the narrow tuning endorsed by a stricter lock-and-key mechanism between the odorant and receptor (Jortner, 2013). The functional significance of this broad or narrow tuning duality is debated, but may contribute to distinct forms of coding. A combinatorial coding scheme might be realized as some studies indicate that most ORs are broadly tuned, such that the presence of an odorant will activate a set of OSNs and its glomerular targets (Jortner, 2013). Ecologically relevant odors may be detected by highly specific (narrowly tuned) ORs, while a combinatorial coding may have evolved to allow a larger representation of odor space

(Andersson et al., 2015). Recent work has however challenged the view of broadly tuned receptors in the OSNs. At least for the moth species *H. armigera* and *H. virescens*, OSNs are shown to be highly specific (Rostelien et al., 2005). Rostelien et al. (2005) reported that a strong response was typically seen to only one primary odorant, while a few chemically related components were able to produce a weak response. A similar narrow tuning has also been shown in *Drosophila melanogaster* (Mathew et al., 2013).

1.1.1 | *Pheromone and plant-odor pathways*

Information about pheromones and plant odorants are found to be mediated by distinct paths in the insect nervous system (Galizia and Rossler, 2010). A labelled-line coding scheme has been proposed for the pheromone system, in contrast to the combinatorial coding realized by the general odor system. While combinatorial coding involves a read out in downstream areas by the specific glomerular pattern of activity evoked by the distinct odorants, a labelled-line system relates to serial connectivity in which information is conveyed in a linear fashion (Galizia and Rossler, 2010). Sex-related behaviours mediated by pheromones work in contrary with interspecific signals, the latter exhibiting an antagonistic effect on attraction. A separation of the two sub-systems devoted to these signal categories has been well documented in several species, including *H. virescens* (Zhao et al., 2014).

1.2 | **The antennal lobe and first-order olfactory processing**

The OSNs, whose cell bodies are located in the antenna, send their axons along the antennal nerve and terminate onto the dendrites of local interneurons and projection neurons (PNs) in the antennal lobe (AL) (Hansson, 1999, Galizia and Rossler, 2010). The synaptic arborizations of OSN axons are circumscribed to spheroidal neuropil structures known as glomeruli, separated by glial cell surroundings (Hansson, 1999). For the majority of insects studied so far, each glomerulus receives input from a single OSN type, and a general principal, "one glomerulus – one receptor" seems to be valid (Martin et al., 2011, Couto et al., 2005). The synaptic organization of the AL network is complex and synapses within distinct glomeruli are typically dyadic, with one presynaptic and two or more postsynaptic elements (Hansson, 1999).

1.2.1 | *Glomeruli in the antennal lobe*

The number of AL glomeruli present varies between species. In different species of Hymenoptera (bees and ants), it is identified 160 to 450 glomeruli, while in locust about a 1000 small glomeruli-like structures called microglomeruli is found (Galizia and Rossler, 2010). In the moth *H. virescens*, 66 glomeruli have been distinguished in males and females (Berg et al., 2002, Lofaldli et al., 2010). However, more recent work on *H. armigera* have identified 78-80 glomeruli in males, which most

likely also reflect the amount present in the related *H. virescens* (Zhao et al., 2016). In male moths, OSNs responding to sex pheromones segregate from non-pheromone-responding OSN upon the entrance of the AL. Pheromone-sensitive OSNs target a male-specific area of typically three to four enlarged glomeruli, known as the macroglomerular complex (MGC) (Berg et al., 2002). It is also identified two enlarged glomeruli at the analogous position in females (Berg et al., 2002). Non-pheromone responding OSNs, tuned to plant compounds, target the much more numerous ordinary glomeruli. Calcium imaging has confirmed the restricted responses of pheromones and plant odors to these two segregated areas (Galizia et al., 2000). Common for all *Heliothinae* species studied, the major pheromone constituent is linked to a specific MGC glomeruli called the cumulus (Berg et al., 2014). The smaller male-specific glomeruli surrounding the cumulus in *H. viresence* are named after their location in respect to the cumulus. In the silk moth *Bombyx mori*, the MGC also have several compartments, named the toroid, cumulus and horseshoe (Sakurai et al., 2014). Bombykol and bombykal, the primary and secondary pheromone component of *B. mori*, are found to have receptor neurons projecting into the toroid and cumulus, respectively (Sakurai et al., 2014).

1.2.2 | *Local interneurons and modulation*

Local interneurons (LNs) are intrinsic cells of the AL that aid in interconnecting the individual glomeruli. In the moth species *Manduca sexta,* both multiglomerular LNs with global (homogenous) branching to almost all glomeruli, as well as oligoglomerular neurons linked to a smaller number of glomeruli have been found (Matsumoto and Hildebrand, 1981, Christensen et al., 1993). The majority of LNs in moths are global and inhibitory, making GABAergic synapses onto both PNs and other LNs in the network (Martin et al., 2011, Hansson, 1999). It has been suggested that LNs contribute a tonic inhibition to PNs, and that a disinhibitory pathway with input from OSNs relieve this PN inhibition, thus mediating their excitation (Christensen et al., 1993). More recent studies illuminate a computationally fundamental role for the LNs, possibly by modulating the overall activity pattern of glomeruli. Such complex network dynamics may for instance allow the existence of point attractors for glomerular activity patterns (elaborated upon in section 1.2.5), or play a role in the precise spike timing of PNs (Galan et al., 2004, Laurent, 2002).

The LN network allow both modulation of the olfactory signal and a concentration-independent representation of the odorants, by for instance enhancing the OSNs output response at low concentrations (Sachse and Galizia, 2003). Integration of numerous glomerular inputs to the LNs enable them to adaptively regulate the response of PNs in relation to the summed input of the AL, by means of global inhibition (Martin et al., 2011). However, modulation of PN activity is not constrained to the effect of LNs. Centrifugal neurons with cell bodies located outside the AL typically target multiple glomeruli (Hansson, 1999). For both *H. virescens* and *H. armigera*, a

multisensory centrifugal neuron, possibly serving a role in modulation of odor-guided behaviours in response to echo-locating bats, has been found (Zhao et al., 2013).

1.2.3 | *The antennal lobe tracts*

Odor information is conveyed from the AL to the protocerebrum by PNs confined as antennal-lobe tracts (ALT). While most PNs are uniglomerular, thus densely innervating a single glomerulus, some are multiglomerular and effected by a wider scope of glomerular input (Galizia and Rossler, 2010). For moths, the PNs have their cell bodies located in three cell clusters in the AL, the lateral cell cluster (LCC), medio-dorsal cell cluster (MCC) and antero-ventral cell cluster (ACC), with the LCC being the largest (Homberg et al., 1988).

A fundamental body of knowledge about the gross anatomy of the ALTs in the hawk moth *M. sexta* was identified by Homberg et al. (1988), in which 5 ALTs were revealed (fig. 1); the medial (mALT), mediolateral (mlALT), lateral (lALT), dorsal (dALT) and dorsomedial (dmALT), following the modern nomenclature of Ito et al. (2014). For *H. virescens*, three of these tracts, mALT, mlALT and lALT (fig 1) have been shown in mass-staining (Ro et al., 2007). Morphologically distinct subtypes of PNs within the different tracts were also observed (Homberg et al., 1988).

The mALT: The most prominent of the described tracts is the mALT. This tract exits the AL as two distinct roots, the dorsal and ventral, and runs medio-ventrally toward the protocerebrum. At the postero-lateral edge of the central body the two roots fuse, and continue together, targeting the mushroom body calyces (MBc), where axonal branches synapse onto the dendrites of the intrinsic MBc neurons, known as Kenyon cells (Homberg et al., 1988). Further, the mALT continues toward the lateral parts of the median protocerebrum, including the lateral horn (LH). In general, the mALT PNs are uniglomerular, while the remainder of the tracts typically show multiglomerular innervations (Homberg et al., 1988).

The mlALT: The smaller mlALT leaves the AL between the two roots of the mALT, and runs along the same route toward the central body, before turning laterally at its edge. Most mlALT PNs terminate in the ventral LH and parts of the superior protocerebrum (Homberg et al., 1988).

The lALT: The lALT is the most neuron numerous tract, however many of these neurons are very small (< 1μm). The tract leaves the AL medio-ventrally, and continue toward the lateral protocerebrum. However, once it reaches the tritocerebrum, the tract looses its definition, as fibres continue in different directions. A small part of the lALT is also found to branch of toward the subesophageal ganglion. Fibres reaching the lateral protocerebrum innervates the LH, before some of these PNs (POc) continue toward the calyces (Homberg et al., 1988, Ro et al., 2007). The lALT runs in a opposite direction compared with the mALT, with the latter innervating the MBc before the LH.

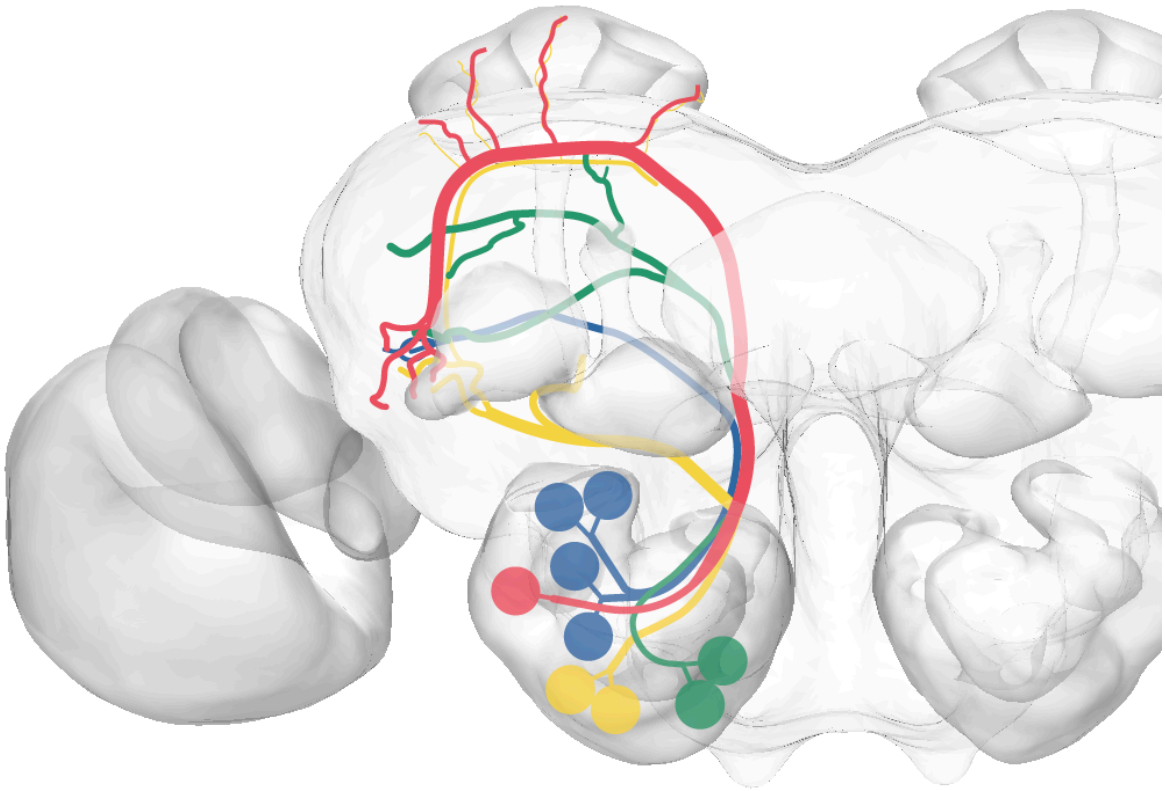

Figure 1 | **Schematic of the major antennal-lobe tracts (ALTs) mediating olfactory information**. The three major ALTs and the tALT projecting from the antennal lobe to higher order areas of the moth brain, superimposed onto the standard brain atlas of H. viresence. Red: mALT. Green: tALT. Blue: mlALT. Yellow: lALT.

The dALT/dmALT/tALT: The previously described dALT and dmALT are not identified by mass-staining in *H. virescens*, however single PNs have been labelled in the dmALT (Ro et al., 2007). The dmALT is suggested to consist of about 16 fibers in *M. sexta*, and is the most dorsal of the tracts, leaving the AL dorso-medially before running postero-laterally toward the MBc (Homberg et al., 1988). In drosophila, and more recently in the moth *H. viresence*, a small tract known as the transverse ALT (tALT) has been described (fig 1) (Tanaka et al., 2012, Ian et al., 2016). The functional role of the tracts is currently not understood.

1.2.4 | *Coding schemes of the antennal lobe*

While *rate coding* is the oldest and most commonly explored form of coding in neuroscience, demonstrated in sensory systems almost 85 years ago by Lord Adrian, modern neuroscience has illuminated other parameters for the encoding of information, however not mutually exclusive from the former (Stein et al., 2005, Adrian et al., 1932). These new parameters include *temporal coding*, where the exact timing of spikes plays a crucial role, and *population coding*, in which the collaborative activity of neurons in an ensemble is able to represent information (Stein et al., 2005, Averbeck et al., 2006).

An hypothesis involving combinatorial population coding of olfactory information has been investigated in both the insect AL, and the homologous olfactory bulb (OB) of mammals and fishes (Galan et al., 2004, Rubin and Katz, 1999, Friedrich et al., 2004). Generally, odorants are shown to elicit patterns of glomerular activation that are stable across multiple presentations of an odorant in the animal, as well as across individuals. These patterns also extend into the temporal domain, in which a consistent pattern of consequently activated glomeruli can be observed with calcium-imaging of the AL (Galan et al., 2004). Similar findings have been seen in the OB in mammals and fishes (Rubin and Katz, 1999, Friedrich et al., 2004). The AL and OB glomeruli have therefore been suggested to encode olfactory information as a spatio-temporal odor map.

To allow animals to distinguish highly similar odorants, mechanisms have developed in which odor discrimination can be achieved through increasing the contrast of the spatial odor map, known as the Mori model (Mori et al., 1999). The model suggests that inhibitory, GABAergic interneurons permit lateral inhibition, thus sharpening the signal. Highly correlated patterns of activity will be observed when comparing the initial activity pattern of AL glomeruli for two similar odorants (Galan et al., 2004). It is suggested by Galan et al. (2004) that attractor network dynamics serve as a pattern separation mechanism in the AL. The temporal evolution of activity in this network will lead to distinct, decorrelated patterns of activity (fig 2A). This decorrelation can be visualized as different trajectories in a vector space (fig 2B), and possibly be read out by downstream targets. The dynamic AL glomerular activity pattern reaches a steady state after about 1 second in honey bees (Galan et al., 2004). Others have suggested a less rigid framework, with more transient dynamics and several semi-stable states (Mazor and Laurent, 2005).

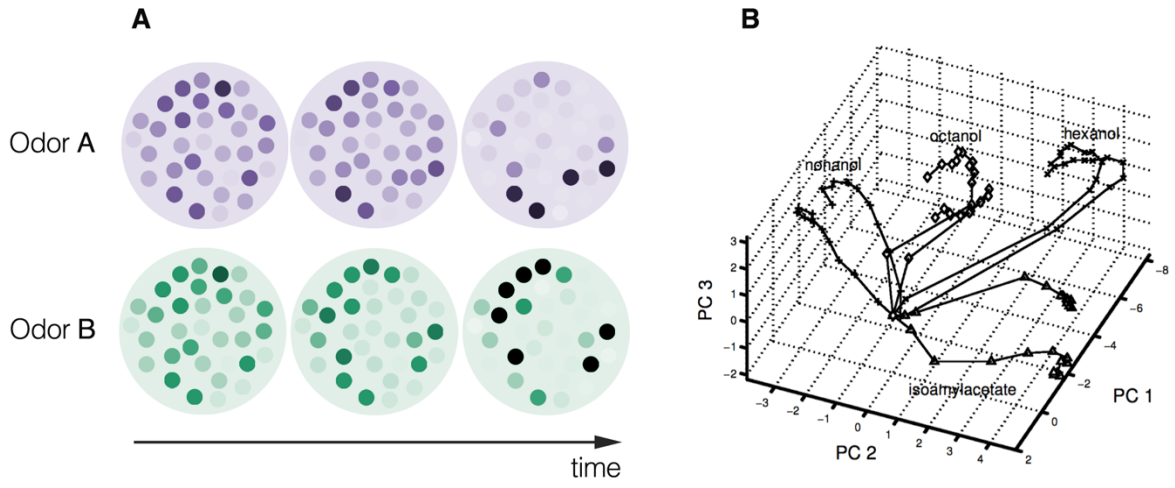

Figure 2 | **Odor-specific vector trajectories of the antennal lobe (AL) activity pattern**. **A)** Simplified drawing of the AL, showing an example where two similar activation patterns of AL glomeruli, one for odor A and one for odor B, are decorrelated over time. **B)** Trajectories are down-projected from 99 dimensions to 3 dimensions using principal component analysis. All odorants begin with similar activity patterns, however as time evolve they become less similar, hence their patterns decorrelate over time. Figure B) is adapted from Galan et al. (2004).

1.3 | **Protocerebral olfactory processing**

In the insect protocerebrum, olfactory information conveyed along the ALTs mainly targets the mushroom bodies calyces and the lateral horn in the lateral protocerebrum (Galizia and Rossler, 2010).

1.3.1 | *Lateral horn*

While the LH has typically been described as a horn-shaped lateral neuropil in the superior posterior brain, modern nomenclature suggests including a larger area in the LH term, covering the greater volume of the insect lateral protocerebrum (LP) that receives AL PN input via the ALTs (Ito et al., 2014). Pheromone responsive projection neurons have been shown to target a distinct sub-region of the LP, namely the delta region of the inferior lateral protocerebrum (ΔILPC) (fig 3B), an area often described as neighbouring the LH inferiorly (Seki et al., 2005). Following modern nomenclature, this region is considered part of the LH (Ito et al., 2014).

The LH is not only a second-order recipient of olfactory information, but is also found to receive innervations from other sensory modalities, including visual and mechanosensory information, both suggested to help insects track odors in flight (Gupta and Stopfer, 2012, Duistermars and Frye, 2010). Generally, the LH is thus considered an integration center that is more closely linked to motoric centers than the MBc (Zhao et al., 2014). Several hypotheses for the functional role of the LH have been put forward and evaluated, including multimodal integration, bilateral processing, involvement in concentration coding and encoding of innate olfactory preferences (Gupta and Stopfer, 2012). While abolishment of the mushroom bodies resulted in deficits of olfactory learning in the fruit fly *Drosophila melanogaster*, innate behaviours guided by olfaction was left mostly intact, indicating a possible role for the LH (de Belle and Heisenberg, 1994).

Jefferis et al. (2007) found that PNs with responses to fruit odors and pheromones were anatomically segregated in the LH of *D. melanogaster,* innervating the posterior-dorsal and anterior-ventral regions, respectively. This suggested a LH topography related to biological values of olfactory input, thus reflecting the segregation observed in the AL glomeruli. Different projection patterns in the LH have been observed in two related moth species, *H. virescens* and *Helicoverpa assulta* (Zhao et al., 2014). Furthermore, in the silk moth *B. mori*, segregation of the two pheromone components bombykal and bombykol have been observed in partly distinct subdivisions of the ΔILPC (Seki et al., 2005). In the honey bee LH, this segregation has allowed predicting the behavioural response to flower odorants (Roussel et al., 2014). Here, 10 morphologically distinct classes of LH neurons have been identified, yet they are not possible to distinguish on the basis of spiking patterns (Gupta and Stopfer, 2012).

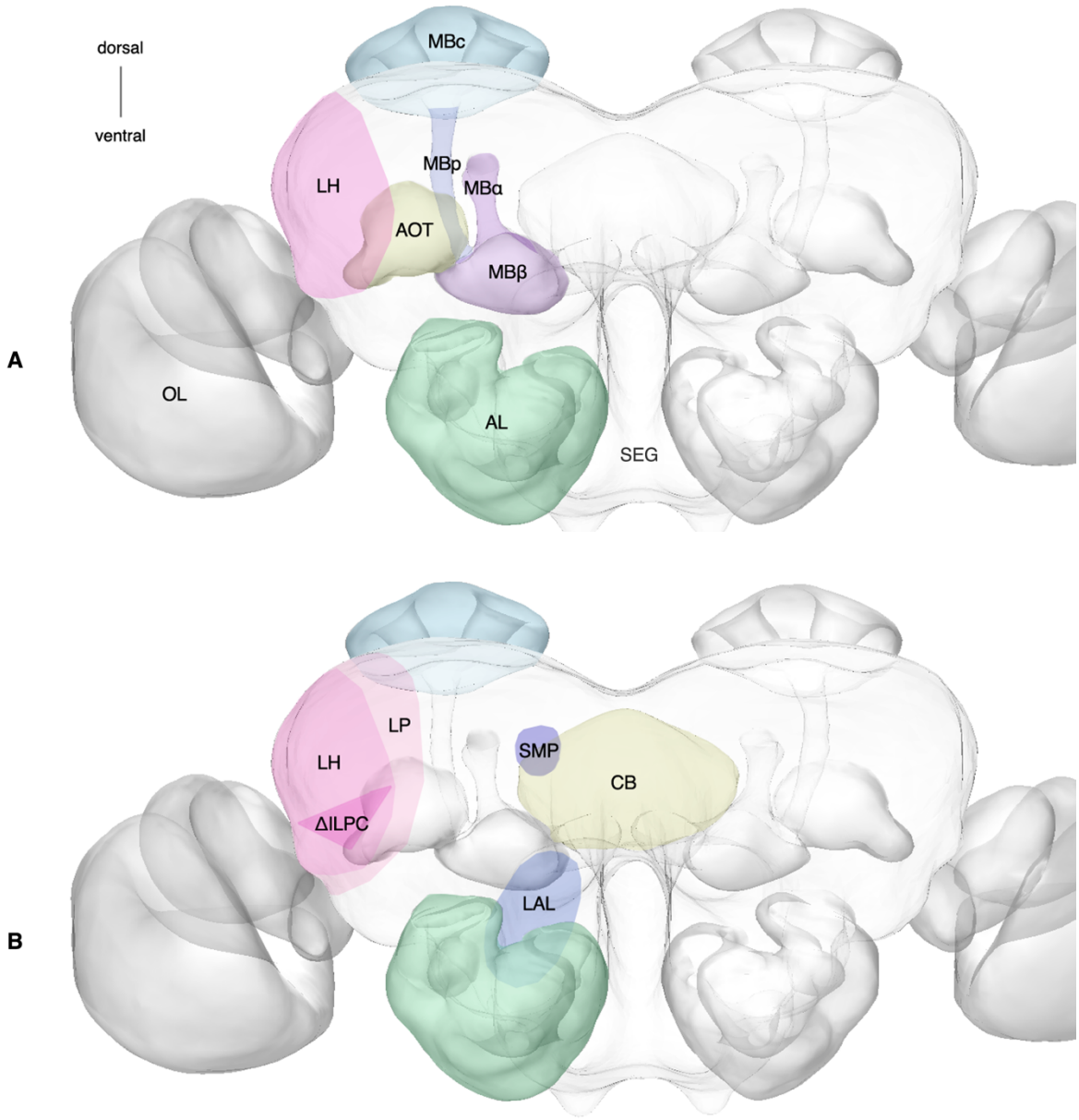

Figure 3 | **Schematic representation of brain areas involved in olfactory processing in the moth.** **A)** Major areas involved in olfactory processing, including the mushroom body areas, the lateral horn (LH) and the antennal lobe (AL). **B)** Areas involved in the neuronal circuitry for pheromonal flow of information as described by Namiki et al. (2014). *AL: Antennal lobe; AOT: Anterior optic tubercle; CB: Central body; ΔILPC: Delta area of the inferior lateral protocerebrum; LH: Lateral horn; LP: Lateral protocerebrum; MBα: Mushroom body alpha lobe; MBβ: Mushroom body beta lobe; MBc: Mushroom body calyces; MBp: Mushroom body penduculus; SEG: Subesophageal ganglion; SMP: Superior medial protocerebrum.*

1.3.2 | *Mushroom Bodies*

Serving an important role in associative learning and memory, the mushroom bodies cover a large area of the brain in most insect species (de Belle and Heisenberg, 1994, Ito et al., 2014). Its high number of intrinsic cells, the Kenyon cells (KCs), are sparsely activated by its input (Martin et al., 2011). Calcium-imaging measurements in honey bees have revealed that about 20% of KCs may be active during an odor stimulation. In honey bees, odors have not been found to be spatially represented in the MBc, contrasting the observations of the AL and LH. Neither do KCs sharing a similar tuning seem to be co-localized in any particular area (Honegger et al., 2011). In moths however, it has been found that pheromone and plant odor information are indeed separated at the input to the MBc (Zhao et al., 2014).

1.3.3 | *Downstream target areas for odor information*

While little is currently known about the third-order neurons originating in the LH and MBc, anatomical studies seem to uncover a distributed system. Tanaka et al. (2004) revealed three constrained target zones for PNs in the LH of *D. melanogaster*, from which third-order projections targeted areas including the superior lateral and superior medial protocerebrum (SLP, SMP), the lateral- and ventrolateral protocerebrum, and the antennal mechanosensory and motor center. In addition, a more recent study has identified a sensory-motor pathway for pheromone information in the moth *B. mori*, in which pheromone information are projected as PNs from MGC to ΔILPC, and third-order neurons to SMP. Projections from SMP target the lateral accessory lobe, before descending interneurons convey the information to the ventral cord (Namiki et al., 2014). Still, these areas are highly interconnected with several other brain regions.

1.4 | **Comparative aspects to the mammalian and human olfactory system**

Mammals, including humans, detect odorants through receptors located in the olfactory epithelium of the nasal cavity, before the olfactory sensory neurons project toward the OB, the mammalian equivalent of the AL (Gottfried, 2010). In both vertebrates and insects, odorants are found to interact with G protein-coupled receptors on sensory cells, yet signal transduction and receptor-types are thought to be fundamentally different, with mammals expressing up to ten times more OR types than what is found in insects (Kaupp, 2010). Yet, striking similarities in the organization of the olfactory system can be observed, for instance with the presence of glomeruli in both the mammalian OB, the insect AL and the homologous olfactory bulb of fishes (Bekkers and Suzuki, 2013, Berg et al., 2002, Friedrich and Wiechert, 2014).

In humans, the olfactory tract extends from the OB and innervates several areas including the anterior olfactory nucleus, olfactory tubercle, piriform cortex, the cortical nucleus of the amygdala

and rostral entorhinal cortex (Gottfried, 2010). Collectively, these regions are sometimes referred to as "primary olfactory cortex", however the same terminology is also typically applied to piriform cortex alone. These regions all receive olfactory information in parallel and show a large degree of reciprocal interconnections (Gottfried, 2010). Subsequently, olfactory information is distributed along several brain regions, including orbitofrontal cortex, hippocampus, hypothalamus, perirhinal cortex, caudal and basolateral amygdala, agranular insula and thalamus, in which the latter allows for olfactory sensory information to reach neocortex (Gottfried, 2010, Galizia and Lledo, 2013).

A distinguished pathway for pheromones and socially relevant odorants as observed in insects is also seen in some mammals, where pheromones are detected by olfactory sensory neurons in the vomeronasal organ, located at the base of the nasal cavity, which target the accessory OB rather than OB (Kaupp, 2010).

1.5 | **Aims and goals**

This thesis serves as a minute part of the ongoing mission at the Chemosensory lab to unveil the anatomy and function of the olfactory system in moths. The principal aim of this thesis is to extend upon this knowledge, by using intracellular recording and iontophoretic staining, in order to characterize the physiology and morphology of neurons in the lateral horn. Using two related *Heliothinae* moth species as a model organism, I will investigate how olfactory information is processed in this higher-order multisensory brain region.

Specific goals:

- Describe the morphology of afferent and efferent olfactory neurons in the LH.
- Characterize response patterns of these neurons to antennal stimulation with biologically relevant stimuli including pheromones and interspecific signals, synthetic plant odorants, and a natural plant odor mixture obtained from sunflower.
- Investigate responses in LH neurons to multimodal stimuli, including both light and odor.

2 | Materials and methods

2.1 | **Insects**

The insects used in the study included males and females of the two related *Heliothinae* moth species *Helicoverpa armigera* (Lepidoptera; Noctuidae, Heliothinae) and *Heliothis virescens* (Lepidoptera; Noctuidae, Heliothinae). *H. virescens* moths were bred in the lab (at 66% humidity and 27°C) from eggs sent by Bayern (Crop science, Germany), while the *H. armigera* moths were bred in China (Henan Jiyuan Baiyun Industry Co., Ltd) and sent to our lab as pupae, already sorted by gender. Male and female pupae were kept separated in two climate chambers (Refritherm 6E and 200, Struers-Kebolab, Albertsund, Denmark). The climate chambers effected a reversed night-day cycle of 14 hours light and 10 hours dark, and held a set temperature of 23°C. Hatched moths were contained as maximum 5 individuals in cylindrical Plexiglas containers (18 x 10 cm) with perforated lids, separated according to species and age. The containers included a paper sheet and a small plastic cup with 10% sucrose solution as nutrition for the moths.

2.2 | **Preparation of test odorants**

The odor stimuli included in total two individual plant odor components, a twelve component plant odorant mixture, four pheromone components (two for each species), a specie-specific pheromone blend, four interspecific pheromones components (two for each species), and a naturally produced volatile plant mixture ("headspace sample") from sunflower (*Helianthus annuus*). Pure hexane was used as control. The odors used for stimulation was diluted in hexane, with plant odors at a 10^{-5} M concentration (10μg/100μl) and pheromones at a 10^{-6} concentration (50ng/100μl). The odorants were applied to individual clean filter papers (diameter = 1.5 cm) at 100 μl for plant odorants (giving 10 μg pure odorant), and 20 μl for pheromones and interspecific signals (giving 10 ng pure odorant), allowing the solution to be distributed throughout the paper. For the headspace sample of sunflower, 20 μl was applied to the filter paper. However, due to the unreliable consistency of the headspace solution, 40 μl was used if the 20 μl of the solution did not fill the filter paper. A weak nitrogen air flow was used to evaporate the hexane, before the filter papers were placed into glass cartridges (length: 11 cm, ID: 0.4cm). The two forcipes used to handle the filter papers during this procedure were heated with a Bunsen burner (30% butane,

70% propane, Plein Air International, Cividale, Italy) after the preparation of each odorant to prevent contamination of the separate odorant cartridges. The glass cartridges were kept in a freezer at (-20°C) and changed after 5 days of use.

All pheromones and interspecific signals used were based on earlier studies (Berg et al., 2014). This included the two interspecific components *cis*-9-tetradecenal (Z9-14:AL) and *cis*-11-hexadecenol (Z11-16:OH) for *H. armigera* and the two interspecific components Z11-16:OH and *cis*-11-hexadecenyl acetat (Z11-16:AC) for *H. virescens*. The species-specific pheromone blend used on *H. armigera* was made by applying a 95:5 ratio of the primary pheromone component *cis*-11-hexadecenal (Z11-16:AL) and secondary component *cis*-9-hexadecenal (Z9-16:AL), respectively, such that a combined 10 ng was used. For *H. virescens* a 96:4 ratio of the primary component Z11-16:AL and secondary component Z9-14:AL, also applied at a total 10 ng amount. The twelve component mixture, blend 12 (B12) (Lofaldli et al., 2012), were applied as 100 μl, thus making a total of 10 μg. The odorants of the B12 mixture included: Hexanol, (3Z)-hexen-1-ol, (3Z)-hexenyl acetat, ocimene, (+)-linalool, geraniol, (+3)-carene, e-verbenol, methyl benzoate, 2-phenylethanol, farsene and (-)-germacrene D. In addition to the B12 mixture, (+)-linalool, (+3)-carene, (-)-germacrene D (from now on referred to as linalool, careen and germacrene D) and geraniol were used as individual stimulants (Table 1). In one preparation, 2-phenylethanol was also used as an individual stimulant. All plant odor components were selected due to their known effect on receptor neurons in *H. armigera* and *H. virescens* (Rostelien et al., 2005).

Table 1 | **Odorants used in the experiments**. Each odorant used is marked as bold. **A)** Components of the plant odor mixture blend 12. **B)** Additional plant odor stimuli used, including two single components and the headspace sample from sunflower. **C)** Pheromones and interspecific signals used for the two species.

A

Blend 12		
(+)-Linalool	Hexanol	Methyl benzoate
Geraniol	3Z-Hexen-1-ol	2-Phenyl ethanol
(+3)-Carene	3Z-Hexenyl acetat	Farsene
E-verbenol	Ocimene	(-)-Germacrene D

B

Sunflower
(+)-Linalool
(-)-Germacrene D

C

	Helicoverpa armigera	*Heliothis virescens*
Pheromone mixture	Z11-16:AL + Z9-16:AL (95:5)	Z11-16:AL + Z9-14:AL (96:4)
Interspecific signal 1	Z9-14:AL	Z11-16:AC
Interspecific signal 2	Z11-16:OH	Z11-16:OH
Primary pheromone	Z11-16:AL	Z11-16:AL
Secondary pheromone	Z9-16:AL	Z9-14:AL

The headspace sample of sunflower was previously obtained by members of the lab by letting a sunflower sit under a ventilated arrangement that collected plant volatiles into a filter. The volatiles were then drained into hexane.

2.3 | **Preparation of insects**

Prior to preparation, the insects were kept for about 5-10 minutes in the refrigerator (4°C) to become sedated and calmed down. The insects were fixed in a plastic tube using dental wax (Kerr Corporation, Romulus, MI, USA) such that the head was exposed with the antennas protruding (fig 4A). A small piece of paper was gently pushed up into the plastic tube to further keep the animal fixed. Using a stereomicroscope (Leica; MZ 12.5) the proboscis was fixed under a piece of dental wax before the cephalic hairs between the antennas were removed using wet paper and a forceps. A fine razor knife was used to remove the cuticle between the eyes of the animal (fig 4B). Intracranial muscles and parts of the main trachea were then removed to expose the brain, before parts of the esophagus was removed. A sharp tungsten needle was used together with a fine forceps to remove the protective sheet covering the brain in the LH area, permitting insertion of the thin glass electrode. Accessible antennal muscles were removed to decrease the movement, and the antennas were further fixated using two needles to keep them in place and lifted up from the wax. Administration of Ringer's solution with sucrose (NaCl: 150mM, KCl: 3mM, TES buffer: 10MM, $CaCl^2$: 3mM, 25mM sucrose, pH: 6.9) was carried out with the use of a plastic pipette throughout the procedure to prevent dehydration of the brain.

2.4 | **Intracellular recording**

The microelectrode used for intracellular recording and iontophoretic staining was composed of a silver-nitrate coated silver wire inserted into a borosilicate glass micropipette, the latter made by means of a Flaming-Brown horizontal puller (P97; Sutter instruments, Novato, CA, USA). Using a preprogramed setting it was possible to ensure similarities of all the electrode tips (Heat: 330, Pull: 80, Velocity: 60, Time: 250), giving the final microelectrodes a resistance of 100-450 MΩ. The glass micropipettes were filled with a fluorescent dye, either dextran tetramethylrhodamine-biotin (Micro-Ruby, Invitrogen, Germany) or dextran fluorescein-biotin (Micro-Emerald, Invitrogen, Germany), and further back-filled with a solution of potassium acetate (0.2 M). A silver wire was inserted into the glass micropipettes and connected to a preamplifier (Axoprobe-1A, Axon Instruments, USA). A silver-nitrate coated silver wire inserted into the hemolymph of the

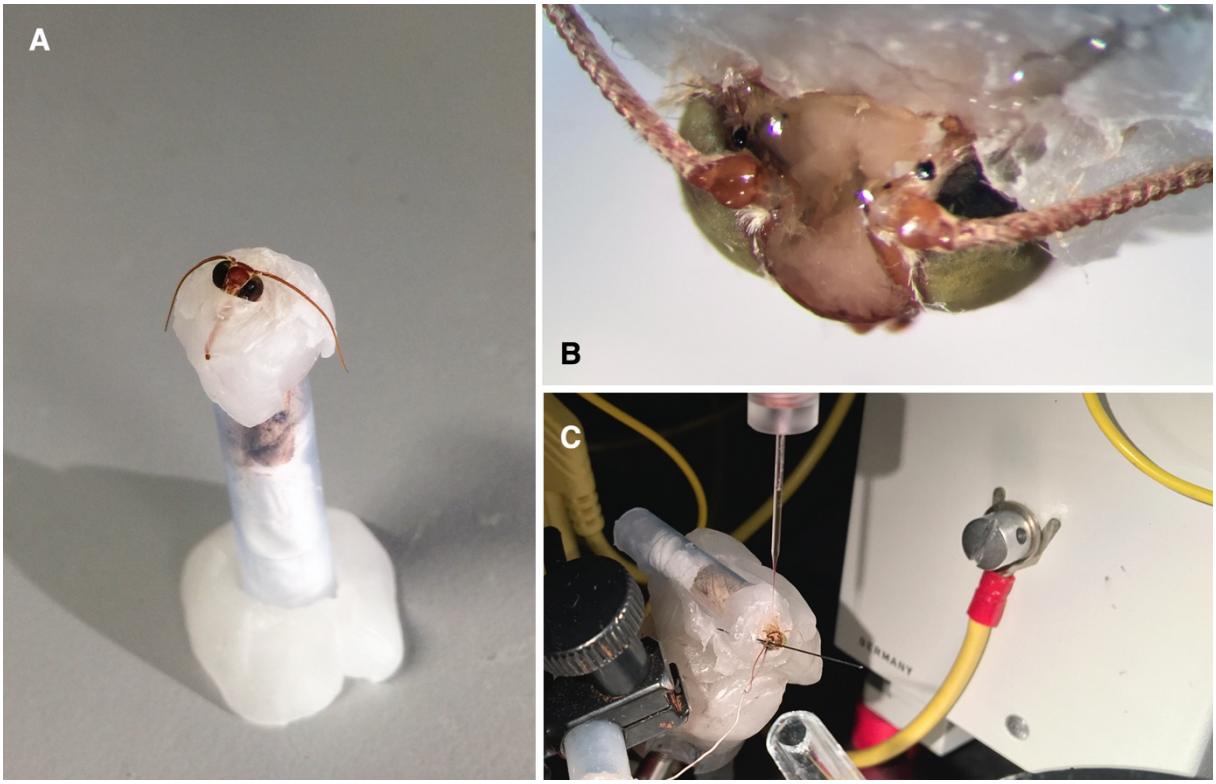

Figure 4 | **Demobilization of insects for intracellular recording**. **A)** The insect is demobilized in a plastic tube with dental wax to fixate its head. **B)** The fur, cuticle and trachea are removed from the head, exposing the brain in a dorsal view. **C)** A glass microelectrode is lowered into the brain to perform intracellular recordings. The clean glass cartridge blowing a continuous air stream toward the antenna can be seen.

right compound eye of the animal was used as a reference electrode, resulting in a current circuitry (fig 4C). Fluctuations in the voltage between the glass electrode and the reference electrode could be monitored on an oscilloscope (Tektronix 5111A, Oregon, USA) and further digitalized using a Micro 1401 mkII data acquisition unit (Cambridge Electronic Design Limited, Cambridge, UK) connected to a computer. A written script running in the software Spike 2 (version 6.14, Cambridge Electronic Design Limited) was used for all data acquisition. Under a microscope (Leica MZ APO), a micromanipulator (Leica) was used to precisely penetrate the neural tissue in the LH area with the microelectrode. Successful penetration of a neuron could be observed as distinct voltage spikes on the oscilloscope and spike 2 software, in addition to be heard in the load-speaker connected to the amplifier (Monacor, MAB-30AK), demonstrating contact with a neuron. During the intracellular recordings, the insect was mounted onto a laboratory table (Micro-g, Technical Manufacturing Corporation, Peabody, MA, USA) to limit vibrations, with a Faraday cage surrounding the setup to exclude electrostatic and electromagnetic influences.

2.5 | Odorant stimulation and iontophoretic staining

A continuous air flow at 500 ml/min was delivered to the right antennae of the animal throughout the procedure via a Teflon tube connected to an empty clean glass cartridge. Upon contact with a neuron, the different odorants were tested. A premade glass cartridge containing an odorant or blend was selected in a pseudorandom manner during each experiment. The odorant glass cartridge was connected to a second tubing system, containing a mechanical valve controlled by the running Spike 2 script, allowing distinct air puffs of 500 ml/min to be delivered at a 400 ms duration upon activation. The odorant glass cartridges were aligned in parallel with the pure air cartridge, with a distance of about 2 cm between the antennae and the positioned cartridges. Each odorant cartridge was pre-labelled with an index letter used as keyboard input to activate the mechanical valve. The different odorant cartridges were changed manually in the tubing system between stimulations, and the selected keyboard letter input allowed linking the odorant used with each stimulus onset. The script compensated for the time-delay from the opening of the valve to the odorant reaches the antenna, which has been calculated to be 200 ms (Høydal, 2012).

Ideally, each of the odorants should be tested, but due to the unstable nature of the electrode's contact with the neuron in this type of recording, not all odorants were tested for all neurons. Where possible, each odorant was tested at least twice to ensure repeatability of the response, usually with a minimum 20 second interval. The control stimulus with hexane was always given to eliminate the possibility of a mechanosensory response. In addition, to investigate multimodal responses in LH neurons, a light stimulus was given with a handheld flashlight.

After the stimulation with different odors, the neuron was iontophoretically stained by passing a 5-12 nA depolarizing or hyperpolarizing current pulse (200 ms, 2Hz), for micro-ruby and micro-emerald, respectively. The passing of the pulse current was continued as long as neuronal activity could be visualized in the oscilloscope, typically for 10-15 minutes.

2.6 | Dissection, fixation and the dehydration protocol

After the iontophoretic staining was completed, the insects were put in a dark, humid container for 3 hours in room temperature, or overnight in the refrigerator (4°C), to let the fluorescent dye get disseminated throughout the neuron by means of axonal transport. Later, under a stereomicroscope (Leica MZ; 12.5), the antennas, palps and proboscis were cut off using a micro-scissor. Next, the insects head was decapitated and fixed in dental wax heated to a melted solution using a soldering iron (ERSA WM 1500 S, Germany), such that the neck region of the animal merged with the wax as the wax cooled down. This allowed for easier dissection of the brain. Ringer's solution was applied throughout this procedure. Once fixed in dental wax, the outer layer

of the two compound eyes was removed using a sharp razor blade to drain the compound eyes of its dark hemolymph, preventing pollution of the brain, before the remaining cuticle of the head capsule that encloses the brain was removed. The brain, with the fully intact eye lobes, was then gently pulled out and put into a small glass container with Ringer's solution, where the brain could be further cleaned using two forcipes. Subsequently, the brain was placed into a 4% paraformaldehyde (Roti-Histofix 4%, Carl Roth GmbH, Karlsruhe, Germany) solution in a small glass bottle for 1 hour at room temperature (20°C) or overnight in refrigerator (4°C). This was done to both fixate the brain and prevent neural tissue degradation. Next, the brain was rinsed in a phosphate buffered saline (PBS, NaCl: 684 mM, KCl: 13 mM, Na2HPO2: 50.7 mM, KH2PO4: 5mM, pH 7.4) for 10 minutes to remove the 4% paraformaldehyde solution, before the brain was dehydrated in an increasing ethanol series (50%, 70%, 90%, 96%, 100%, 100%) with each step for a period of 10 minutes. Replacement of each substance during this process was aided by a plastic pipette, draining the current substance from the glass bottle before the next was applied. After the dehydration protocol, the brain was made transparent by use of methyl salicylate (methyl 2-hydroxybenzonate) and finally ceiled in a methyl salicylate bath between two glass microscope slides on a punctured aluminium plate. The aluminium plate aided the mounting of the brain in the confocal laser scanning microscope.

2.6.1 | *Intensification*

Intensification of the staining was performed if only a weak staining was observed during confocal microscopy. The brains were rehydrated in a revers alcohol series with 10 minutes for each step (100%, 100%, 96%, 90%, 70%, 50%), and rinsed for 10 minutes with PBS, before a 2 hour incubation in streptavidin-Cy3 (1:200 in 0.1 M PBS pH 7.2), all at room temperature (20°C). Subsequently, the brains were again rinsed with PBS for 10 minutes, before and yet again dehydrated in an increasing alcohol series and soaked in methyl salicylate as described above.

2.7 | **Confocal microscopy and neuron reconstruction**

The mounted brain preparations were visualized in a confocal laser scanning microscope (Zeiss LSM 510 Meta, Jena, Germany) at the Department of Biophysics and Medical Technology, NTNU. Micro-ruby stained neurons could be visualized using a helium neon laser, operating at a 543 nm wavelength, to excite the tetramethylrodamine component, while micro-emerald were visualized using an argon laser at 488 nm, exciting the fluorescein. Both a 10x (10x/0.3, Plan-Neofluar) and 20x (20x/0.5, Plan-Neofluar) dry lens objective or a 40x (40x/1.2w, Plan-Neofluar) water objective was used during scanning, dependent on the area of interest. The images were taken at 1024 x 1024 or 2048 x 2048-pixel resolution with a pinhole size of 1 airy unit. The small size of

the moth brain permitted a whole-brain scanning, creating a stack of images. Successfully stained neurons were visualized using the LSM 510 projection tool, and neurons of particular interest were reconstructed using the Skeleton Tree plug-in in Amira 3D (version 5.3.3, FEI, Visualization Science Group). Final adjustments of the images were done using Adobe Photoshop CS6.

2.8 | **Spike data analysis**

2.8.1 | *Preliminary analysis criteria*

During the preliminary analysis, the neuron recordings were visually investigated in Spike 2, of which those fulfilling the following preliminary criteria were selected for further analysis:

1. The neuron had to show response to at least one of the tested substances.
2. The neuron had to be tested with a control stimulus (pure hexane).
3. Each stimulus had to be tested at least twice to ensure consistency.
4. Repeated stimuli had to occur at no less than a 20 second interval.

2.8.2 | *Spike sorting*

Spike sorting was done using the WaveMark tool in Spike 2 (version 6.4, CED), where the continuous waveform recording of spikes for each neuron was converted into a discrete event vector. In the cases where several different spike amplitudes and waveforms were observed, these were treated as distinct neurons and analysed accordingly. Discretized spike trains were exported as 50 ms time bins along with the stimulus onset and stimulus-type events into Microsoft Excel, where a database was compiled for analysis.

2.8.3 | *Response classification*

All neurophysiological data analysis was done using MATLAB (2014b, MathWorks, Inc., Natick, MA, USA), in which a custom-made script allowed for processing and visualization of the data. A response window was defined for each odor stimulus as the period between stimulus onset and the first bin where the following 400 ms did not deviate significantly from the estimated spontaneous activity prior to the given stimulus. Thus, a dynamic response window was defined following each stimulus onset of a neuron recording. A limit was set to 4000 ms to prevent unrealistically long response windows, for instance, in the cases where a stimulus radically altered the spontaneous activity for the remainder of the experiment. The mean firing frequency and variance of the spontaneous activity was calculated for each stimulus on each neuron recording, from the 1500 ms time window prior to stimulus onset.

The mean deviation (in firing frequency) from the estimated spontaneous activity (MDS) was used to quantify the temporal response strength for each response window:

$$MDS = \frac{1}{n}\sum_{i=1}^{n} \left| r_i - r_{sp} \right| \quad (1)$$

where n is the number of time bins, r_i is the firing rate of bin i and r_{sp} is the average firing rate of the calculated spontaneous activity. To estimate the response window, the absolute value of the deviation was used as in (1). An odor response was defined as significant if the MDS in the response window exceeded the standard deviation of the estimated spontaneous activity by a factor of two. Due to the diversity of responses seen in the recorded neurons, neurons that were not considered significant through examining the estimated response window were also tested with a fixed 400 ms response window. This allowed the detection of brief responses with large degrees of noise. To classify the response type, the contribution of the positive (eMDS) and negative (iMDS) deviations was calculated separately. A response was classified as excitatory if at least 80% of the MDS contribution during the response window was excitatory, or inhibitory if at least 80% of the MDS contribution was inhibitory. In the cases were both eMDS and iMDS contributed to less than 80%, a response was classified as complex.

2.8.4 | *Response strength analysis*

The maximum firing rate, within a 2500 ms time window after stimulus onset, was estimated for each response deemed significant according to the analysis criteria stated above. To improve the temporal resolution of the frequency estimation, and to eliminate the arbitrariness of bin placement, the firing rate was estimated by applying a 100 ms sliding rectangular window function to the spike train data. Such a function allows a better estimation of the instantaneous firing rate along the spike train than a binned approach (Dayan and Abbott, 2001) (fig 5C). The firing rate is thus estimated as the average firing rate of a 100 ms window surrounding the point of interest. By sliding this 100 ms window along the spike train at 1 ms steps, the instantaneous firing rate is estimated at each point along the whole spike train (fig 5C).

2.8.5 | *Response duration analysis*

Response durations were subjectively estimated by visually inspecting the spike trains. This was done to determine the differences in response duration for consecutive stimulations of one odorant.

2.8.6 | *Inter-spike interval analysis*

To investigate the difference in patterns of spontaneous activity in LH neurons, inter-spike interval (ISI) histograms were created for each neuron (see fig 5). Discretized spike trains were exported as 1 ms time bins from Spike 2, and used for generation of ISIs in a custom-made MATLAB script. The plotted ISIs histograms were based on the first 2500 intervals estimated in each neuron recording.

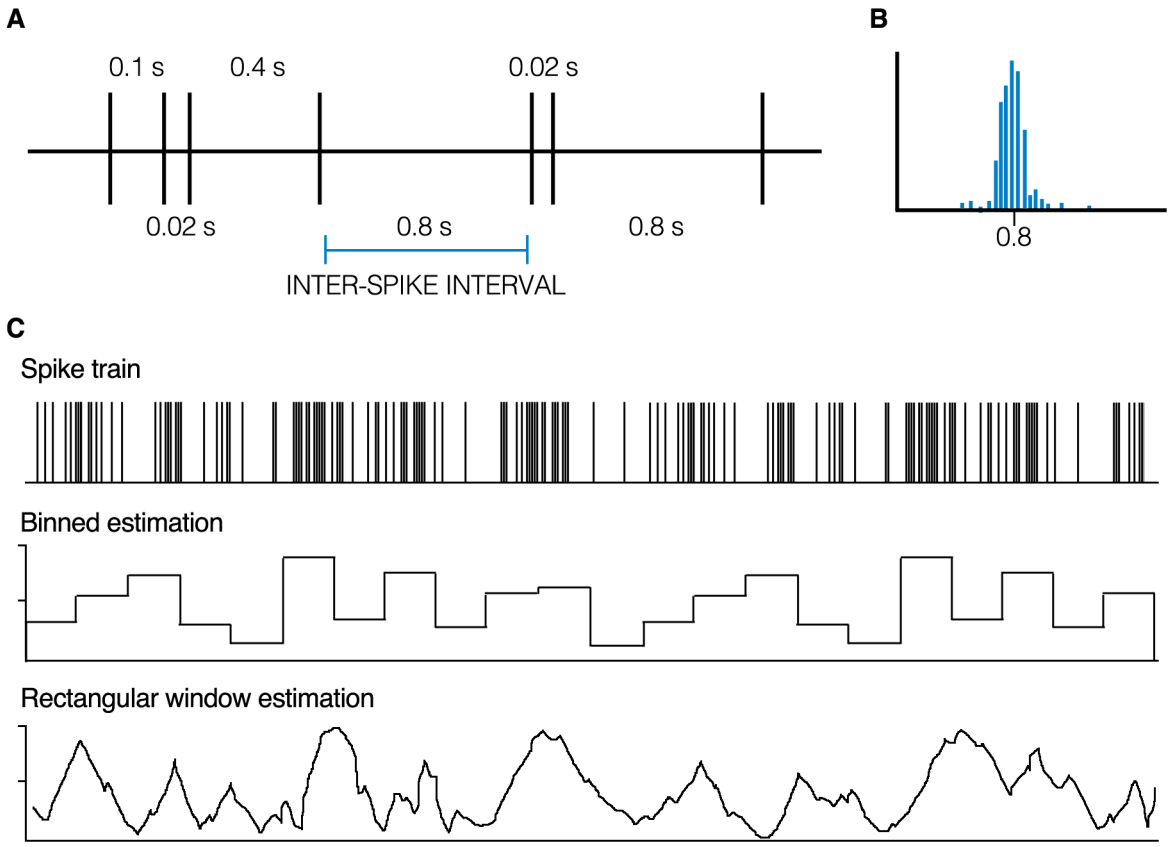

Figure 5 | **Inter-spike interval and the rectangular window function**. **A)** The time interval between each spike is calculated and counted, such that a histogram can display the spike number of each interval. A highly regular spiking neuron would give a high count around one interval length. **B)** Regular firing will be reflected as a sharp peak in the histogram. **C)** A sliding rectangular window function was used to get a better estimation of instantaneous firing rate, compared to a binned estimation. Each point in the estimation is the result of sliding a rectangular window over the spike train, giving each point along the x-axis the value of the mean activity in a 100 ms window surrounding the given point. Figure C) is based on Dayan and Abbott (2001).

2.9 | **Ethical considerations**

Whether insects feel pain, and to what extent, is a debated question. Nonetheless, nociceptive sensitization has been demonstrated in the larvae of the moth species *M. sexta*, and it is generally accepted that alternative mechanisms might subserve a function of pain perception in non-nociceptive insects (Walters et al., 2001, Eisemann et al., 1984). Additionally, a recent study reported that agitated honey bees display altered behaviours and reduced hemolymph levels of several modulatory neurotransmitters, suggesting that negative emotional states might exist in some invertebrates (Bateson et al., 2011). While some arthropods, like honey bees and decapods, are protected by the Norwegian law of animal welfare (*Lov for dyrevelferd*), there are currently no restrictions in the use of Lepidoptera for experimental research. In spite of this lack in lawful restrictions, the insects used in this study were cared for, and surgical procedures were carried out, in a manner that reduced any unnecessary harm or stress. Additionally, the chambers containing insects were attended to on a daily basis. This to ensure that sufficient amounts of nutrients were provided, and that the general milieu was satisfactory for their wellbeing.

3 | Results

A total of 63 neuron recordings were obtained from 50 of the 115 insect preparations that were used in this study. Of these 63 neurons, 21 (N1-N21) showed a significant response to antennal stimulation with at least one odorant. Successful stainings were achieved from 10 neurons linked to the LH, distributed on five individuals (preparation 1 to 5; p1-p5) (Table 2). In total, 41 neurons across 29 individual insects were subjects for staining attempts. The 10 stained neurons were all reconstructed (R1-R10) to better visualize their morphological characteristics.

Table 2 | **Summary of experimental results**

	H. armigera	***H. virescens***	**Total**
Number of animals (males/females)	98 (95/3)	17 (13/4)	115 (108/7)
Mean days of age	8.8	7.7	8.6
Number of attempted stainings	28	13	41
Number of successfully stained preparations	3	2	5
Number of stained neurons innervating LH	7	3	10
AL projection neurons in the mALT	3	1	4
AL projection neurons in the mlALT	0	2	2
AL projection neurons in the dmALT	1	0	1
Higher order neurons	2	1	3
Successful (attempted) stain with micro-ruby	7 (23)	2 (7)	9 (30)
Successful (attempted) stain with micro-emerald	0 (8)	0 (3)	0 (11)
Recordings obtained	50	13	63
Number of recordings used for analysis	17	4	21

One preparation showed an accidentally stained AL interneuron. This neuron was not included in the results, but its remarkably beautiful morphology, and its physiology, is presented in the appendix (A1)**.** Additionally, one preparation displaying a staining in about 14 neurons confined to the protocerebral-calycal tract was obtained, but not presented in the results. The morphology of this preparation can also be seen in the appendix (A2).

3.1 | **Physiological characteristics of the neurons**

Recordings obtained from neurons in the LH revealed a great diversity in both spontaneous activity (fig 6) and response breadth (fig 7).

3.1.1 | *Spontaneous activity*

A generally high spontaneous activity, most often ranging from 20 to 80 HZ (fig 6), was observed among the 21 responding neurons. A substantial diversity in spike regularity, as demonstrated by the inter-spike interval histograms, could also be seen (fig 6A). Some similarities among the ISI histograms were present, yet no apparent correlation between odor response or morphology and ISI histogram shape could be seen. A shift in spontaneous activity was seen in some neurons.

3.1.2 | *General response patterns*

The response breadth of most neurons in the LH was found to be broad, meaning that one neuron responded to several odor stimuli, as shown in figure 7. Most responses were shown to be excitatory, while only a handful neurons showed complex responses. The majority of neurons were found to display different response patterns to different odor stimuli, either as complex or excitatory. Only one neuron showed a significant inhibitory response to an odor stimulus. Response to a light stimulus was seen in four of the 21 odor-responsive neurons (19%) (fig 7). All light-responsive neurons showed a flat ISI histogram shape.

The headspace sample from sunflower was found to elicit an odor response most often. In 17 of the 19 tested neurons (89%), a response was observed for sunflower, all excitatory (table 3). The second most potent odor stimulus was the primary pheromone component, followed by the ideal pheromone mixture and the secondary pheromone component. While the ideal pheromone mixture induced an excitatory response in all responding neurons, the primary and the secondary pheromone component alone was found to elicit a complex response. The single plant compound germacrene D did not show a significant response in any of the neurons tested.

Table 3 | **Occurrence of odorant responses**. Each odorant is sorted according to the % of responses elicited. Responses to a light stimulus is also shown.

Odorant	Nr. neurons	Nr. Responses	% Responding	% Excitatory	% Complex	% Inhibitory
Sunflower	19	17	89 %	100 %	0 %	0 %
Pri. phero. comp.	5	3	60 %	66 %	34 %	0 %
Pheromone mixture	21	12	57 %	100 %	0 %	0 %
Sec. phero. comp.	7	4	57 %	50 %	50 %	0 %
Blend 12	20	11	55 %	82 %	9 %	9 %
Control	21	10	47 %	60 %	40 %	0 %
Interspecific signal 2	9	3	33 %	66 %	34 %	0 %
Linalool	16	5	31 %	100 %	0 %	0 %
Interspecific signal 1	13	3	23 %	66 %	34 %	0 %
Germacrene D	4	0	0 %	0 %	0 %	0 %
Light	21	4	19 %	25 %	0 %	75 %

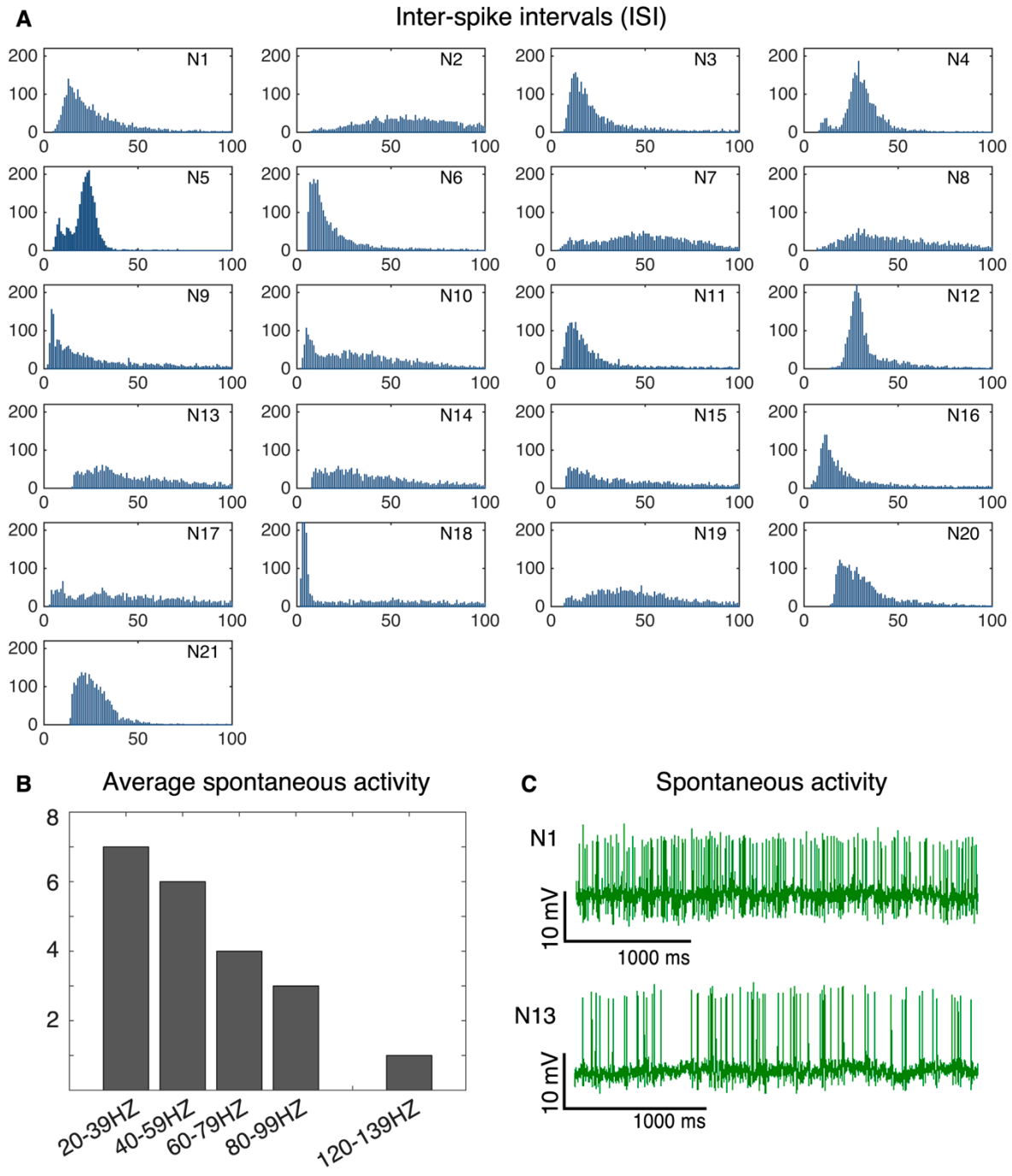

Figure 6 | **Inter-spike intervals and spontaneous activity**. **A)** Inter-spike intervals (ISI) were estimated for all 21 neurons. The *x*-axis shows intervals in a range between 0 to 100 ms, and the *y*-axis the count. **B**) Histogram depicting the spontaneous activity bandwidth across the 21 neurons. *Y*-axis shows the number of neurons. **C)** Lack of regularity in spiking, as in N13, gives a flat ISI histogram in A).

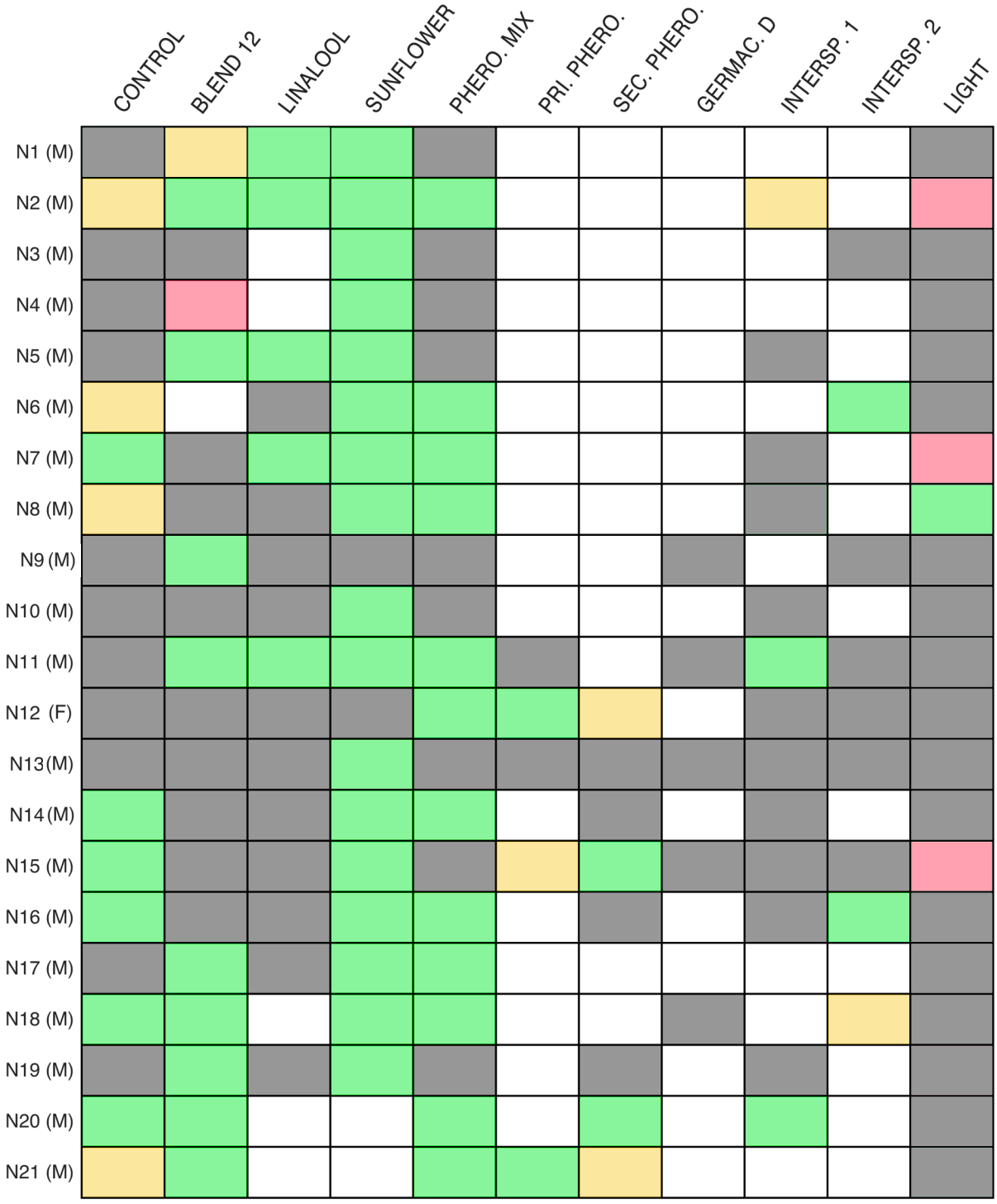

Figure 7 | **Response profiles of individual neurons**. Analysis of spike frequencies during stimulation, estimated with a custom-made MATLAB script, proved a significant response in 21 of the 30 neurons included in the physiological analysis (N1-N21). N12 is the only responding neuron recorded from a female. Green = excitatory response; yellow = complex response; red = inhibitory response; grey = no response; white = not tested.

Visual inspection of the spike trains did however reveal alterations from spontaneous activity for germacrene D in some neurons. Interestingly, the only neuron obtained from a female in the neurophysiological data used (N12) responded exclusively to pheromones.

The maximum firing rate (MFR) during a response was estimated from a 2500 ms time window following stimulus onset. The MFR differed in the 21 neurons, yet the rates were consistent for consecutive responses to a particular odorant for the majority of neurons (fig A3, appendix).

Response durations

Based on the fact that most neurons responded to several of the tested odorants, it was relevant to investigate whether individual neurons might differentiate between stimuli by varying the length of the responses. Response durations according to particular stimuli were estimated for eight neurons showing significant responses to both the pheromone mixture and sunflower, and to the control and/or linalool. The average response durations to the four stimuli were estimated in all eight neurons, based on the spike trains observed during the first two exposures of each stimulus. As shown in figure 8, the response durations to the various stimuli differed substantially for some of the neurons. Only two neurons, N2 and N7, showed negligible differences. N8 showed on average a slightly longer response to pheromone than control, however this is also considered negligible. N6, N16 and N18 however, showed a much longer average response to sunflower and the pheromone mixture than to the control. For N18, the difference in response duration between control and sunflower was about 1600 ms.

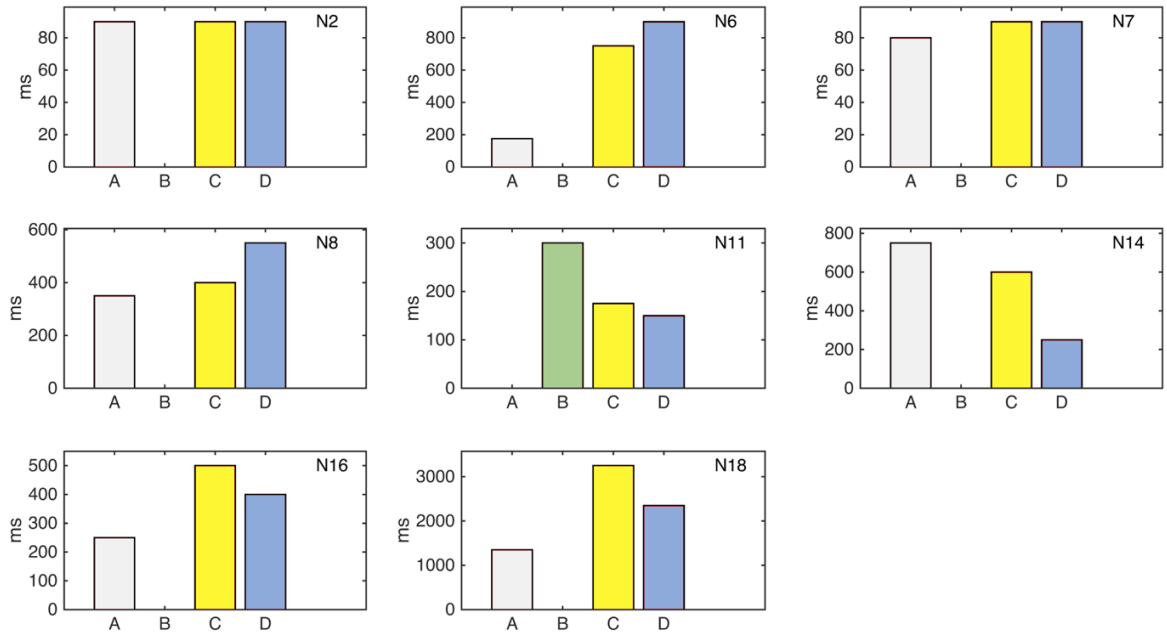

Figure 8 | **Response duration**. The figure shows the average response duration of the two first stimulations for control (A), linalool (B), sunflower (C) and the ideal pheromone mixture (D), for 8 neurons showing response to both pheromone and sunflower, and control or linalool. N6, N16 and N18 show a much longer average response to sunflower and the pheromone mixture than the control.

The response duration for sunflower in N18 was much longer for the first stimulation (4500 ms) than the second stimulation (2000 ms) (fig A4, appendix). N11 showed an average longer response duration to linalool than sunflower and the pheromone mixture (fig 8), while N14 showed an average longer response duration to control, compared to the sunflower and the pheromone mixture.

In addition, consecutive trials of sunflower stimulation led to different response durations for sunflower in N3 and N18 (fig 9). In N3, an oscillatory background firing could be seen (fig 9A).

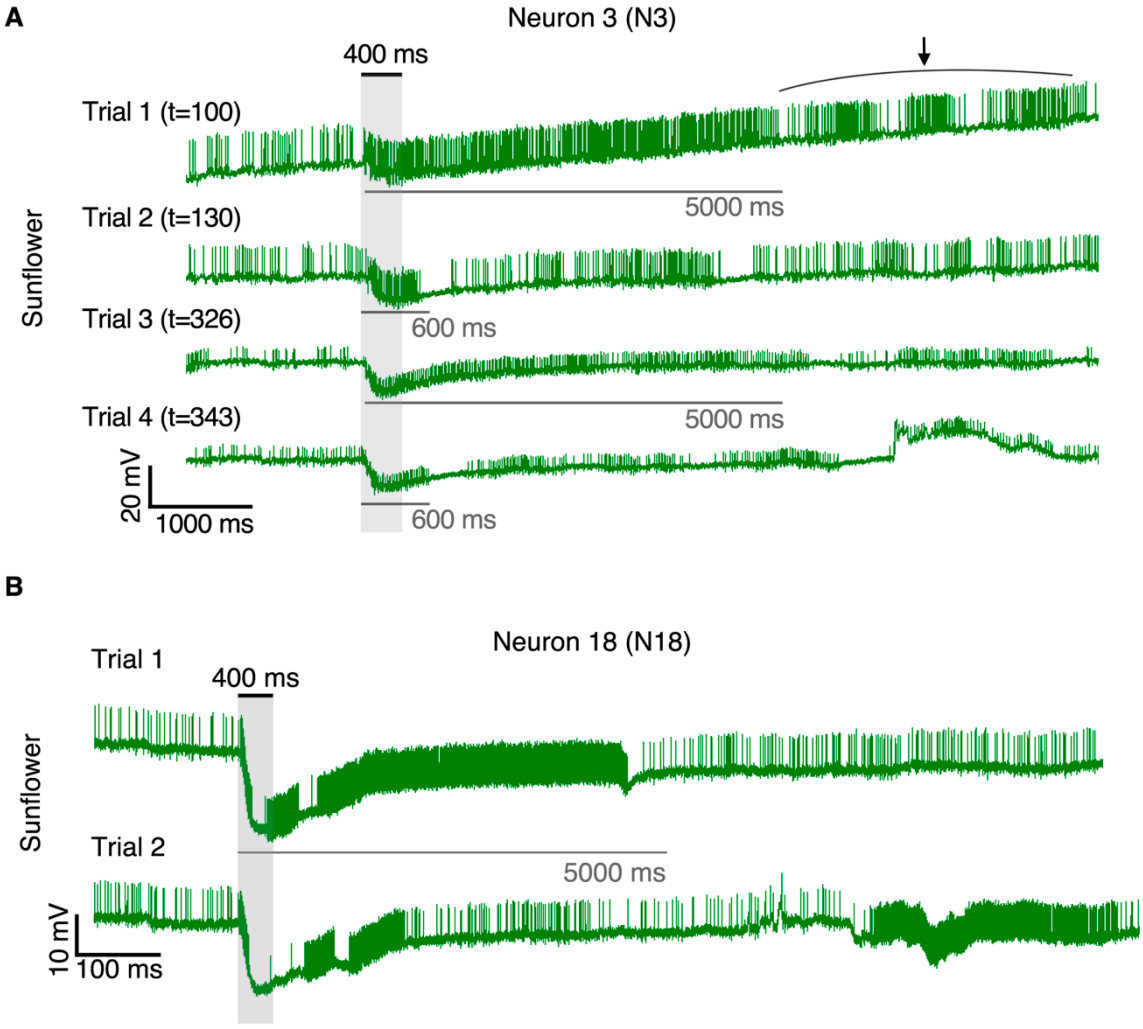

Figure 9 | **Trial-dependent responses**. **A)** In N3, when presented with two subsequent stimulations of sunflower at a 30 second interval (trial 1 and 2), the response length was decreased with almost a 10-fold. 200 seconds later, an identical response pattern was again observed for two subsequent stimulations. Arrow in trial 1 shows a repeating oscillatory background firing that could be seen in the neuron throughout the recording. **B)** Responses for two consecutive trials of sunflower in N18. **A-B)** Stimulus onset is shown as grey bar. Onset time for stimulus within the neuron recording is shown in brackets behind trial number.

3.2 | **Morphological and physiological properties of the stained neurons**

A total of ten stained neurons, originating from five preparations, were found to innervate the LH. Seven of these were antennal-lobe PNs (shown in p1-p3), four passing in the mALT, two in the mlALT and one in the dmALT. The three remaining neurons were higher-order neurons. In preparation 4, two neurons innervating the LH were simultaneously stained, of which one seemed to be a protocerebral interneuron, and the other possibly a third- or fourth-order olfactory neuron. Preparation 5 showed one stained neuron with large innervations in the optic lobula plate and LH, extending projections to multiple additional regions, including the contralateral LH.

All neurons of interest were reconstructed and *transformed* into the standard brain atlas (SBA) of *H. virescens*, to better visualize and examine their morphological characteristics. Because the two preparations of *H. virescens* (p2 and p5) were deformed, and no such atlas is available for the species *H. armigera*, the reconstructed neurons was not *registered* into the SBA. Table 4 summarizes the characteristics of the ten reconstructed neurons (R1-R10).

Table 4 | **Summary of reconstructed neurons**. All neurons of interest were reconstructed to better visualize and examine their innervations. *ILP = inferior lateral protocerebrum; LH = lateral horn; LOp = lobula plate; MCC, LCC, ACC = medial-, lateral- and anterior cell body cluster; SEG = subesophageal ganglion; VLPC = ventro-lateral protocerebrum.*

Reconstruction	Neuron type	Preparation	Figure nr.	Colour in figure	Somata location
R1	*Projection neuron (mALT)*	p1	Fig. 11	Red	ACC
R2	*Projection neuron (mALT)*	p1	Fig. 11	Yellow	MCC
R3	*Projection neuron (mALT)*	p1	Fig. 11	Blue	MCC
R4	*Projection neuron (mALT)*	p2	Fig. 13	Black	MCC
R5	*Projection neuron (mlALT)*	p2	Fig. 13	Green	LCC
R6	*Projection neuron (mlALT)*	p2	Fig. 13	Red	LCC
R7	*Projection neuron (dmALT)*	p3	Fig. 15	Red	SEG
R8	*Protocerebrum to SEG*	p4	Fig. 17	Red	SEG
R9	*Protocerebral interneuron*	p4	Fig. 17	Green	ILP
R10	*LOp to contralateral LH*	p5	Fig. 19	Red	VLPC

3.2.1 | *Preparation 1*

Data from preparation 1 (p1), a 14 days old male *H. armigera*, included both neurophysiology (fig 10) and morphology (fig 11).

Morphology

Five to six AL projection neurons, all passing in the mALT, had been stained in this male preparation. As shown in figure 11A, these medial-tract PNs innervate the MBc before terminating in the LH. Also, typical uniglomerular arborizations in the AL are visible in the confocal image. Three of these neurons (R1-R3) displayed a stronger staining, and were possible to separate by means of 3D reconstruction (fig 11B and D). All three neurons reconstructed showed uniglomerular innervations in the AL, and two of them, R2 and R3, showed to innervate the same glomerulus. The cell bodies of R2 and R3 were located in the medial cell cluster (MCC), while the cell body of R1 was found in the smaller anterior cell cluster (ACC) (fig 11C). A second stained cell body in ACC was also seen (fig 11C). This latter neuron was not reconstructed, but is most likely among the other stained mALT neurons. It was not possible to identify which of the two cell bodies in the MCC were possessed by R2 and R3 respectively. However, a difference in size could be seen (8 µm and 20 µm). The cell body of R1, which was located in the ACC, was ~20 µm. R7 seemed to have a larger innervation in the LH than R6, extending from the posterior to the anterior part. Because the tip of the electrode had broken off and was still left in the brain, an overexposure of the dye was present in the projection from MBc toward the LH. As a result, only two neurons (R2 and R3) were possible to separate at the entrance of the LH.

Physiology

The recording demonstrated an excitatory response to the single plant component 2-Phenylethanol, which was tested only on this particular preparation. A response was also seen to B12. However, due to the loss of contact with the neuron, B12 was tested only once. An inhibitory response was seen for the remainder of tested odorants, including the control and ideal pheromone mixture. The recording from p1 is not included among N1-N21.

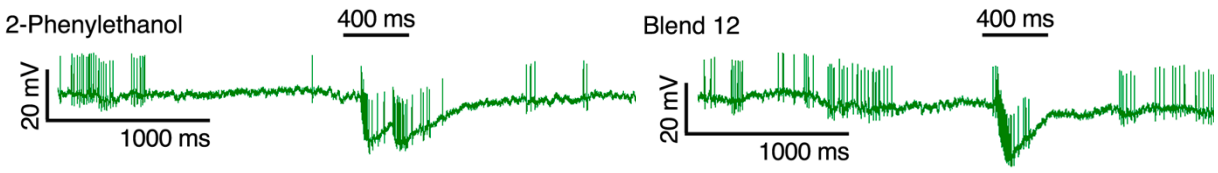

Figure 10 | **Neurophysiology of preparation 1**. The recording obtained from p1 included an excitatory response to stimulation with the single plant odor component 2-Phenylethanol and to blend 12.

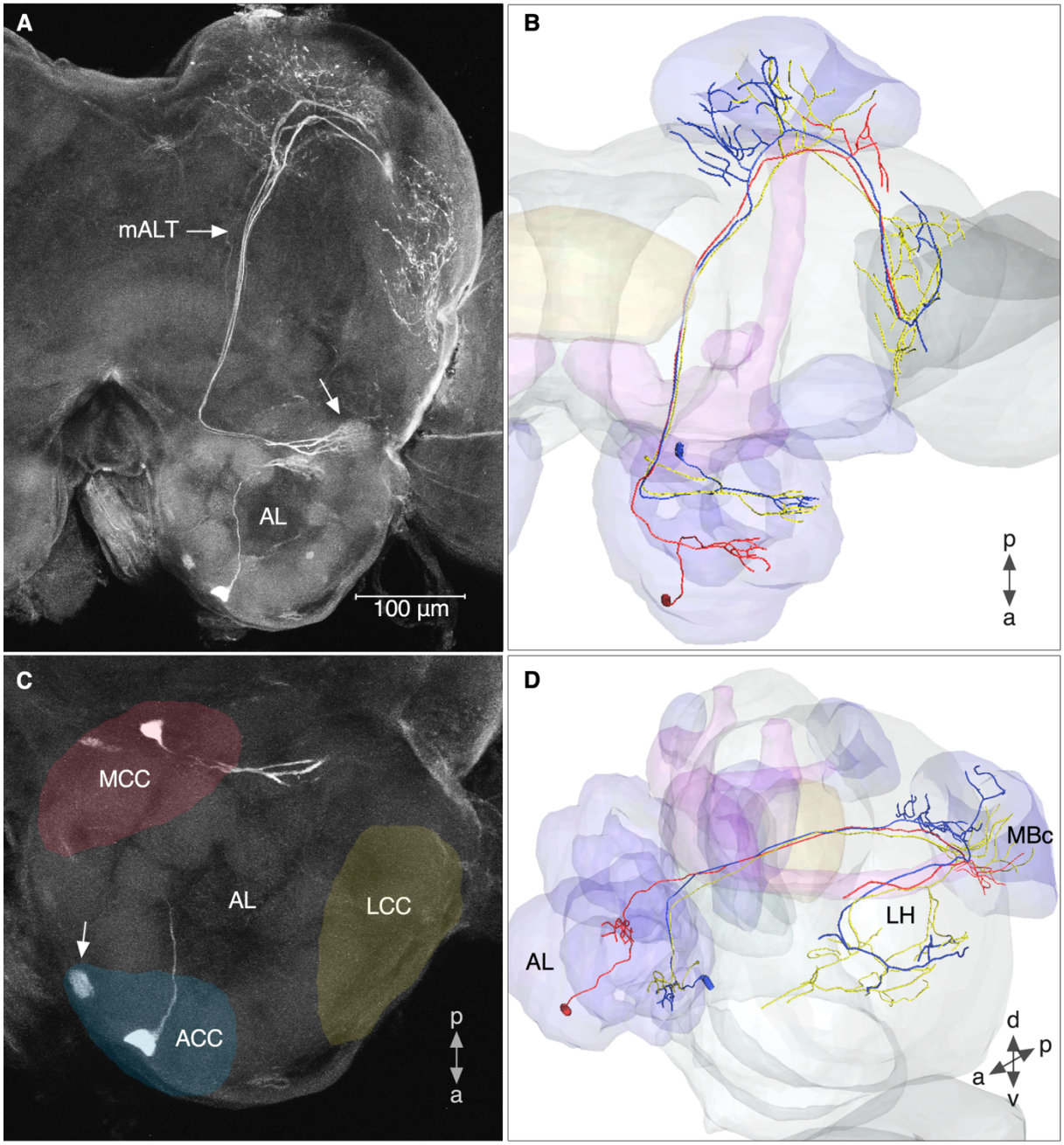

Figure 11 | **Morphology of preparation 1**. **A)** Confocal imaging revealed that 5-6 neurons in the medial antennal-lobe tract (mALT) were stained. White arrow indicates a single glomerulus innervated by two neurons, R2 and R3. **B)** Three of the neurons in mALT were possible to distinguish and could be reconstructed and transformed into the standard brain atlas (SBA) for *H. virescens* for better visualization. R1 (red), R2 (yellow) and R3 (blue). **C)** Colour overlays indicating locations of the medial, anterior and lateral cell body clusters (MCC, ACC, LCC) in the antennal-lobe (AL). The cell body of R1 was located in the ACC, while R2 and R3 had their cell body in the MCC. White arrow indicates a second cell body in the ACC. This neuron was not reconstructed. **D)** Side-view of reconstructed neurons transformed into the SBA. *a = anterior; d = dorsal; p = posterior; v = ventral; AL = antennal lobe; LH = lateral horn; MBc = calyx.*

3.2.2 | *Preparation 2*

Data from preparation 2 (p2), a 14 days old male *H. virescens*, included both neurophysiology (fig 12) and morphology (fig 13).

Morphology

Three AL projection neurons were stained, one confined to the mALT (R4, black) and two to the mlALT (R5, green and R6, red) (fig 13). The mALT neuron was found to innervate the mushroom body calyx before reaching the LH, while the mlALT neurons projected directly to the LH. All three neurons shared an overlapping region in the LH. However, the two neurons passing the mlALT targeted partly different regions in the LH; R5 innervated a larger and more superior-medial region than R6 (only one thin branch of R6 could be seen in this area) (fig 13E). In the AL, both mlALT neurons seemed to have widespread innervations, but R5 was found to innervate more extensively in the ventral-posterior part of the AL than R6.

Physiology

The recording obtained in p2, which is named N11, showed a broad tuning profile (fig 7). Because three neurons were stained, it is not possible to state which neuron the recording originated from. However, since the recording showed such a broad tuning profile, and the two neurons in the mlALT did show a stronger staining than the neuron confined to the mALT, it is reasonable to assume that any of these two neurons represents N11. According to the response analysis, the neuron in recording N11 responded significantly to both B12, the pheromone mixture, Z11-16:AC (an interspecific signal for *H. virescens*), sunflower, as well as the single plant component linalool. Some examples can be seen in figure 12. The neuron showed quite sparse spontaneous activity, with bursts of activity, making a mean of 22 HZ (lowest 16 HZ, highest 35 HZ).

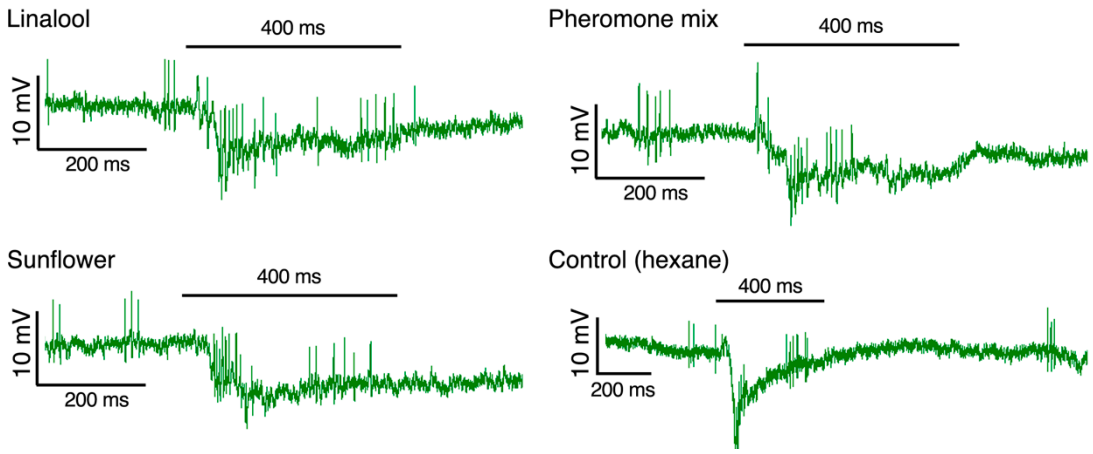

Figure 12 | **Neurophysiology of preparation 2.** Some of the significant responses are included. The spontaneous activity of the neuron was quite sparse, with sudden bursts of activity. The response tuning of this recording is shown as N11 in figure 7.

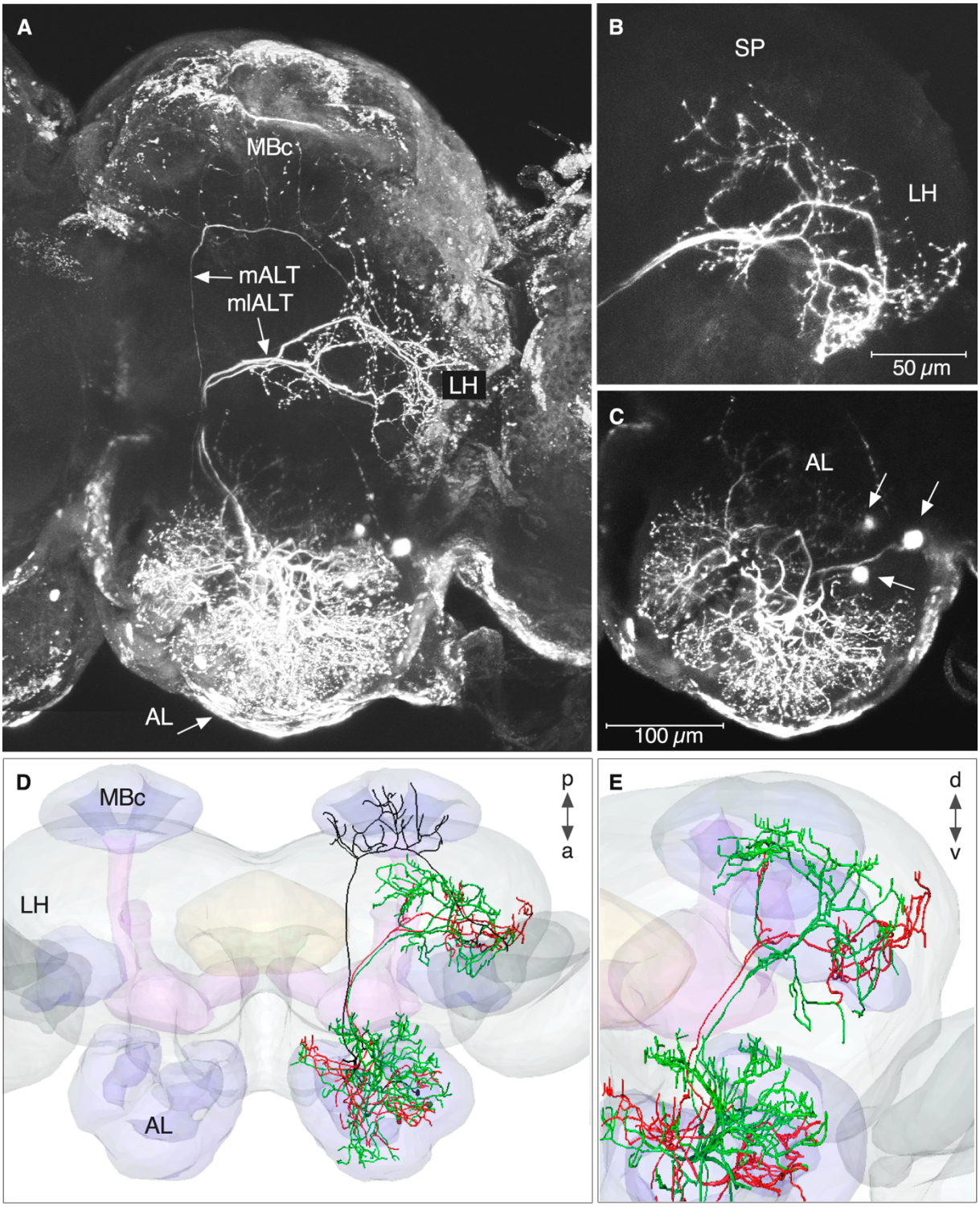

Figure 13 | **Morphology of preparation 2**. **A-C)** Staining of the three antennal-lobe projection neurons (PNs) as obtained by confocal microscopy. **D)** Dorsal view: 3D reconstruction of the PNs, one in the mALT (R4, black) and two neurons in the mlALT (R5, green and R6, red) transformed into the standard brain atlas for *H. virescens* (dorsal view). The green mlALT neuron displays a more medial innervation area in the protocerebrum than the red one. **E)** 3D-reconstruction in a more frontal view: The green mlALT neuron innervates more superiorly than the red mlALT neuron. *a = anterior; d = dorsal; p = posterior; v = ventral; MBc = calyx; SP = superior protocerebrum.*

3.2.3 | *Preparation 3*

Data obtained from preparation 3 (p3), a two days old male *H. armigera,* included both physiology (fig 14) and morphology (fig 15) of one single antennal-lobe projection neuron confined to the dmALT.

Morphology

The bilateral neuron innervated both hemispheres, however the projections in the hemisphere contralateral to the recording site were stained only weakly. The neuron showed uniglomerular innervations symmetrically in the two ALs (fig 15C), and a cell body located medially in the subesophageal ganglion (SEG) (fig 15B). In the ipsilateral hemisphere, the projection toward MBc and further to LH could easily be seen. At the entrance of the LH, the projection splits to innervate both the anterior and posterior regions. In the contralateral hemisphere, the projections seemed to follow an almost symmetrical route. However, beyond reaching the medial protocerebrum, no further projections could be seen. In each hemisphere, the axon passed along the dmALT, which projects dorsally and medially of the mALT. The neuron was reconstructed (R7) and transformed into the SBA of *H. virescens* for a better visualization (fig 15D and E).

Physiology

Due to the conservative response classification used to create the response profiles in figure 7 (see section 2.8.3), the neuron stained in p3 did not show a significant response and is thus not included among N1-N21. Yet, visual examination of the responses indicated that the neuron was indeed affected (fig 14). A consistent inhibition was observed for two trials of Z9-14:AL (interspecific signal 1 for *H. armigera*). For the ideal pheromone mixture (Z11-16:AL and Z9-16:AL) and control (hexane), only a small inhibition was seen. B12 created a consistent complex response in two trials, with a brief inhibition, followed by a burst of activity, and again a brief inhibition. No response was observed when stimulating with Z11-16:OH (interspecific signal). A mean spontaneous activity of 43 HZ was estimated (lowest 22 HZ, highest 62 HZ). Spontaneous activity was estimated on average activity in a 1500 ms window prior to every stimulus onset.

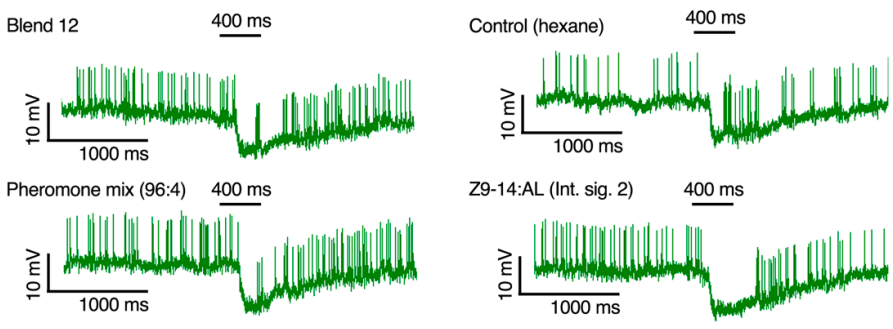

Figure 14 | **Neurophysiology of preparation 3**. Consistent changes in activity were seen when stimulated with B12, Z9-14:AL (an interspecific signal) and the ideal pheromone mixture. However, the responses were not classified as significant according to the criteria specified in section 2.8.3.

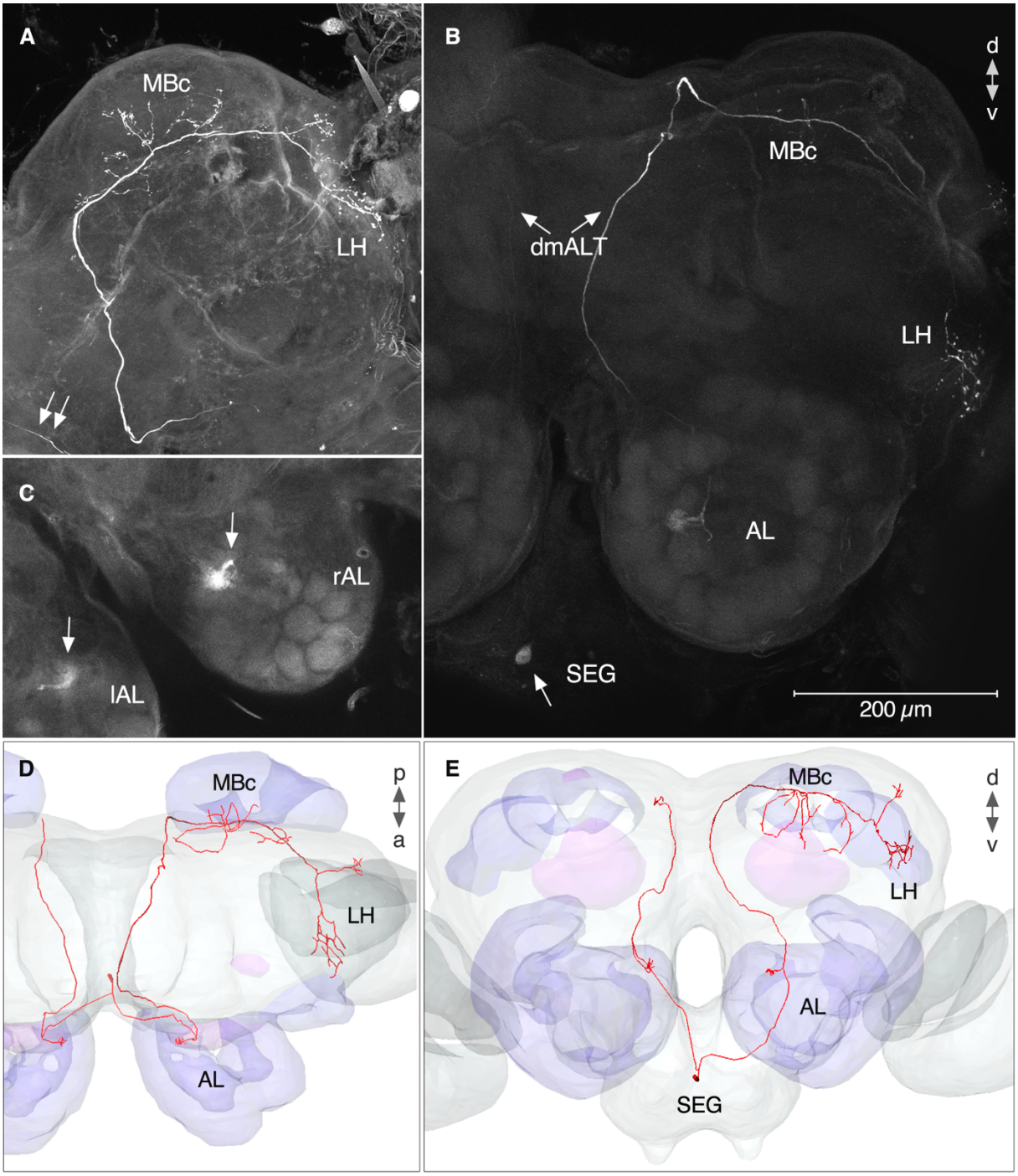

Figure 15 | **Morphology of preparation 3**. One bilateral projection neuron confined to the dorsomedial antennal-lobe tract (dmALT) was stained. **A)** Confocal imaging showing clear innervations in the mushroom body calyx (MBc) and the lateral horn (LH) in the ipsilateral hemisphere. Double arrows indicate the symmetrical projection in the contralateral protocerebrum. **B)** Overview of the bilateral neuron including the stained cell body in the subesophageal ganglion (SEG), the two axons projection in the dmALT (arrows; weakly stained in the contralateral hemisphere). **C)** Symmetrical uniglomerular innervations can be seen in the antennal-lobes (ALs). **D-E)** The reconstructed neuron was transformed onto the standard brain atlas (SBA) of *H. virescens*. *a = anterior; d = dorsal; p = posterior; v = ventral; lAL = left antennal lobe; rAL = right antennal lobe.*

3.2.4 | *Preparation 4*

Data obtained from preparation four (p4), a six days old male *H. armigera,* included both physiology (fig 16) and morphology (fig 17).

Morphology

In p4, three neurons were stained, of which two innervated the LH (fig 17A). The latter two neurons were possible to differentiate and were reconstructed. One of these (R8) sent widespread branches to a large region of the medial, superior, and lateral protocerebrum, including the LH. The cell body of R8 was located laterally in the SEG. A projection running along the peduncle toward the anterior part of the protocerebrum could be seen. Here, the neuron turned medially at the lateral accessory lobe and continued toward the SEG of the contralateral hemisphere. In the SEG, axonal arborizations innervated a larger area, before a projection went further down into the SEG. As the preparation was cut at the top of the ventral nerve cord, it could not be established how far down the neuron continued. The cell body of the smaller R9 neuron was located in the inferior LP. R9 showed only small innervations, mostly in the lateral superior protocerebrum. This neuron is most likely stained as a result of dye leakage across gap junction connections with R8.

Physiology

Due to the strong staining of neuron R8, plus its wide-spread innervations, it is reasonable to assume that the large spike amplitudes (4 mV) measured belong to this particular neuron. The neuron recording is shown as N7 in figure 7. Examples of odor responses can be seen in figure 16. The recorded neuron also responded with a burst of activity when a light source was switched off.

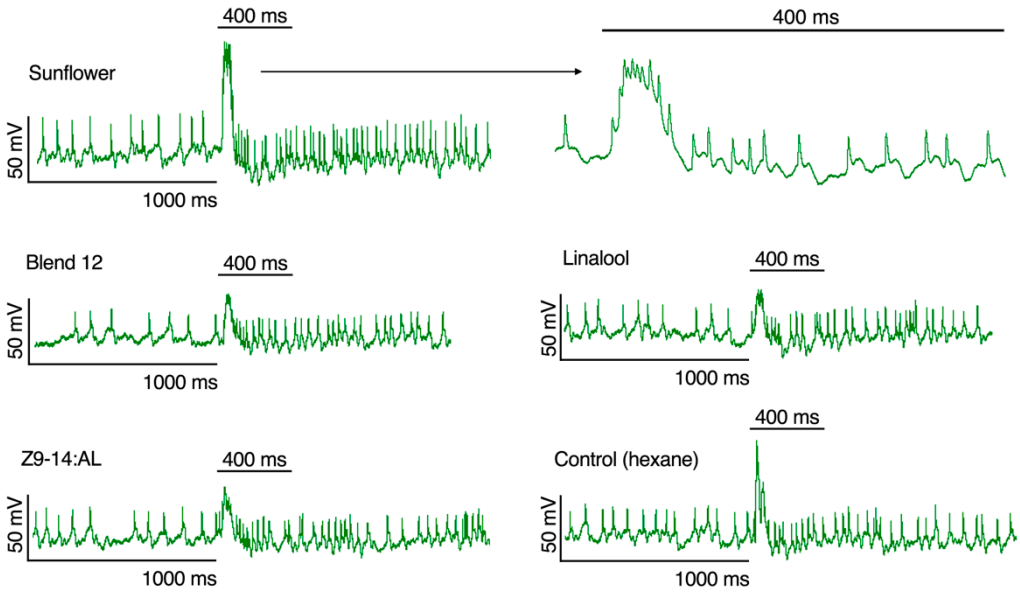

Figure 16 | **Neurophysiology of preparation 4.** Some of the responses obtained from preparation 4. Linalool, hexane, sunflower and the ideal pheromone mixture were all classified as significant according to the algorithmic response classifier.

Preparation 4

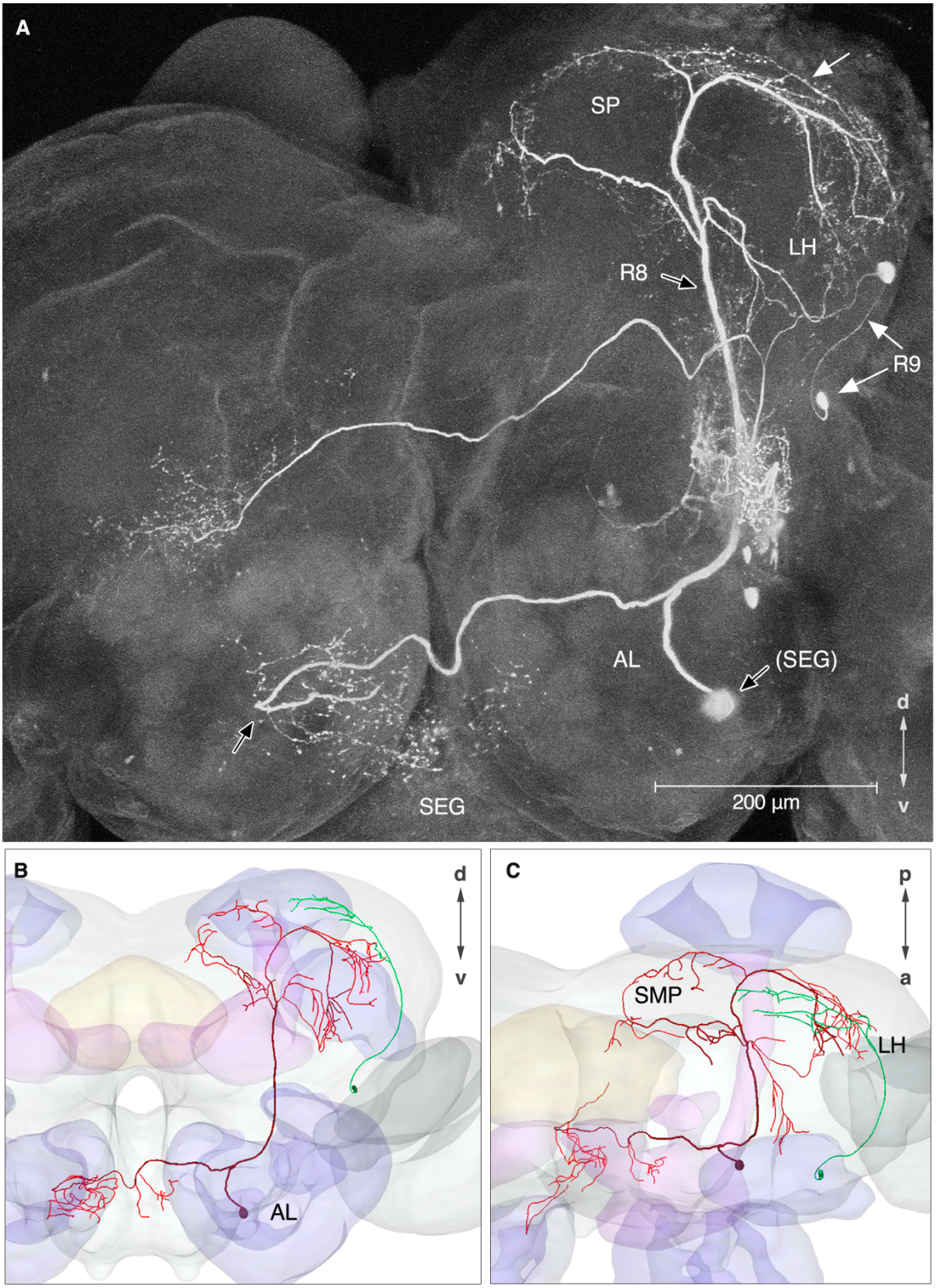

Figure 17 | **Morphology of preparation 4**. Higher order neurons innervating the lateral horn (LH). **A)** Confocal image showing three stained neurons, two of which innervated the LH. Black arrows indicate neuron R8, white arrows indicate neuron R9. **B-C)** 3D-reconstruction of the two LH neurons transformed onto the standard brain atlas (SBA) of *H. virescens*. R8, red and R9, green. *a = anterior; d = dorsal; p = posterior; v = ventral; SEG = subesophageal ganglion; SMP = superior medial protocerebrum.*

3.2.5 | *Preparation 5*

Data obtained from preparation 5 (p5), an 11 days old male *H. virescens,* included both physiology (fig 18) and morphology (fig 19) of a single neuron innervating large areas of the protocerebrum, including the lateral horn and the optic regions.

Morphology

The bilateral neuron extended widespread branches into the posterior part of the brain, connecting the optic lobula plate with both the ipsi- and contralateral LH (fig 19). Upon entrance to the contralateral protocerebrum, the neuron turned to run ventrally along the peduncle, extending several blebby protrusions, before turning laterally into the LH. Innervations were also seen in the ventromedial neuropils, most likely in the posterior slope. Because of the slightly deformed brain, it is hard to determine the specific region of innervation. The cell body (~20 µm in size) was located in the posterior-ventral part of the lateral protocerebrum.

Physiology

Significant responses were seen for the ideal pheromone mixture for *H. virescens,* sunflower, and control (hexane) (fig 18). The neuron responded with brief increases in activity when exposed to these stimuli. B12 and Z11-16:AC were also tested, but did not elicit any deviation in activity. An excitatory response was also seen when a light stimulus was presented. Data from the recording obtained from p5 is shown as N8 in figure 7.

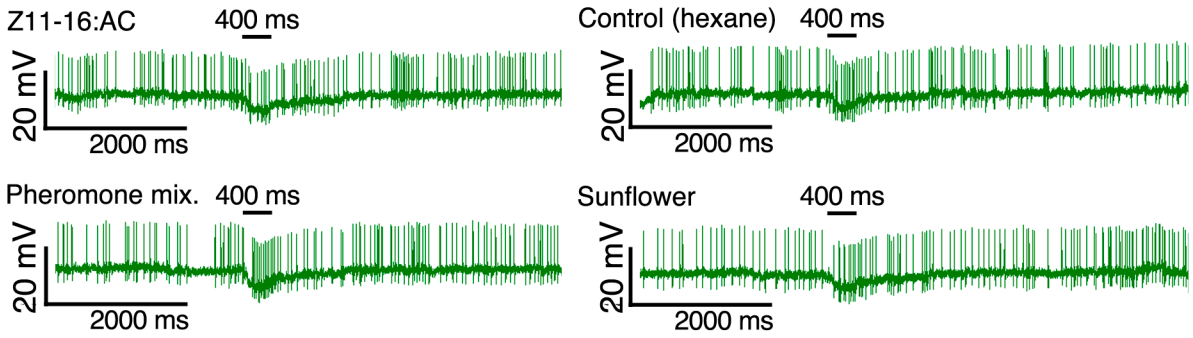

Figure 18 | **Neurophysiology of preparation 5**. The recording (N8) showed a significant response to the ideal pheromone mixture, sunflower, and the hexane used as control. The interspecific signal Z11-16:AC did not affect the spiking.

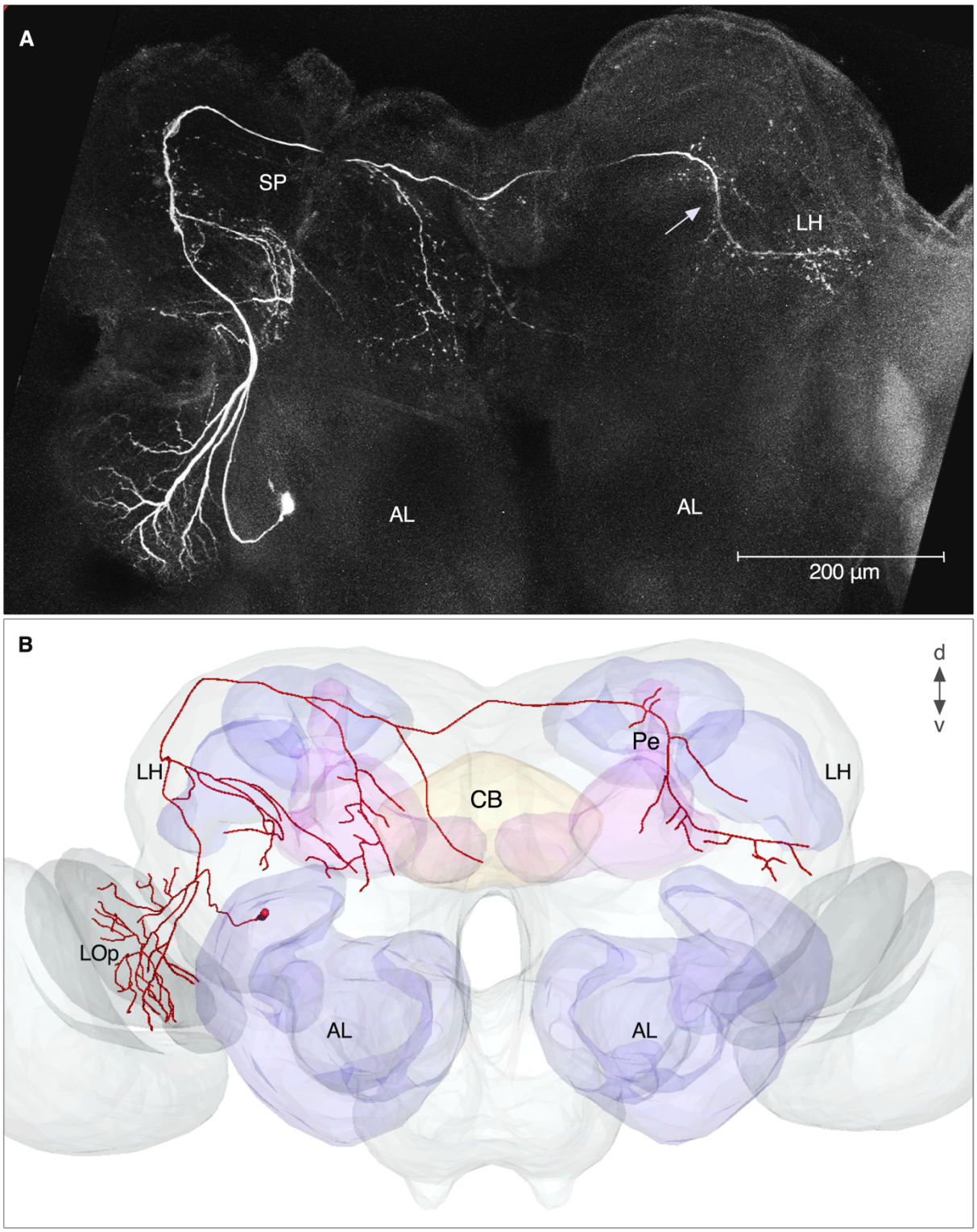

Figure 19 | **Morphology of preparation 5**. Bilateral neuron innervating the lateral horn (LH) and parts of the optic lobe. **A)** Confocal image showing innervations in the lobula plate, the LH and ventromedial neuropils in the ipsilateral hemisphere, as well as in the LH of the contralateral hemisphere. Because parts of the brain had slipped out the opening made in the neural sheet, the stained neuron was slightly disfigured. White arrow indicates the neuron's track along the peduncle. **B)** The disfiguration was corrected for in the 3D reconstruction when the neuron model was transformed onto the standard brain atlas of *H. virescens*. *d = dorsal; v = ventral; AL = antennal lobe; CB = central body; Pe = peduncle.*

4 | Discussion

In order to understand the functional role of the lateral horn in olfaction, it is necessary to map the morphological and physiological properties of input and output neurons in this higher-order brain area. The thesis presented here has examined the neurophysiological responses of LH neurons during antennal stimulation with several different odors, and in addition identified the morphological characteristics of a subset of these neurons. Moreover, a light stimulus was consequently tested in neurons that responded to odor stimuli in order to identify multimodal integration. The physiological data, obtained via intracellular recording, revealed that neurons in the LH are most responsive to naturally occurring odor mixtures, such as headspace samples from sunflower, and the ideal pheromone mixture produced by the female of the same species.

Successful staining allowed morphological characterization of seven antennal-lobe PNs, and three higher-order neurons, all innervating the LH. Physiological data was also obtained from the stained preparations. In addition to complementing previous findings, the results of this thesis contribute new findings concerning the properties of higher-order neurons, as well as second-order PNs confined to the ALTs.

4.1 | **Input to the lateral horn**

The LH receive olfactory input directly from the antennal lobe via PNs forming several parallel ALTs. The functional role of the individual tracts conveying this information is still not fully understood. Seven such PNs, distributed across three distinct ALTs, were stained during the experiments conducted for this thesis.

4.1.1 | *Projection neurons in the mALT and mlALT*

Neurons in the mALT, the most prominent of the tracts, were stained in both preparation 1 and 2. The morphological characteristics of these neurons are similar to previously described mALT PNs in both *Heliothinae* and other moth species (Zhao et al., 2014, Kvello et al., 2009, Valderhaug, 2015, Stav, 2014, Lofaldli et al., 2010, Lofaldli et al., 2012, Homberg et al., 1988, Namiki et al., 2014). All mALT PNs stained and presented in this thesis had uniglomerular innervations in the AL, sent direct projections toward the MBc, and subsequently to the LH. One of the mALT PNs in p1 was found to have its somata located in the small anterior cell cluster, a finding which to my knowledge has not been previously described in *Heliothinae* moths. This is however found in the moth species

B. mori and *M. sexta* (Namiki and Kanzaki, 2011, Sun et al., 1997). Two cell bodies in the anterior cell cluster could be seen in the confocal images of the present study (fig 11C), and one of the stained neurons being connected to these somata, R1, was possible to reconstruct. The two remaining mALT projection neurons, R2 and R3, which were also reconstructed, had their somata located in the lateral cell cluster. Notably, neuron R1 projected to a slightly different region of the MBc as compared to R2 and R3. Thus, while R1 innervated the lateral part of the MBc, R2 and R3 was found to innervate the central and medial most part. Because of the weak stain in p1, these findings might however not necessarily reflect the true innervations of the neurons. In the LH, only R2 and R3 could be reconstructed. Here, R2 was found to target the largest area, stretching from the posterior to anterior most part of the LH. R3, in comparison, showed only thinner branches, innervating the posterior and middle region of the LH. The fourth stained uniglomerular PN confined to the mALT (R4 from p2) showed extensive innervations in the whole of the MBc, contrasting the sparse innervations seen in R1-R3. However, it was not possible to reconstruct R4 beyond the entrance of the LH.

The two reconstructed PNs confined to the mediolateral ALT (R5 and R6) showed widespread multiglomerular innervations in the AL, and were found to innervate in a partly overlapping region of the LH. Neuron R5 also showed innervations in the more superior regions of the protocerebrum, medially to the LH, where only a small branch from neuron R6 was seen (fig. 13).

The region of the LH innervated by the mALT neurons in p1 were found to overlap with the multiglomerular PNs confined to the mlALT from p2 (fig 20). Such an overlap is also seen in mass-staining of the ALTs in *M. sexta* (Homberg et al., 1988). Given the present data, one can only speculate about the functional role of such a configuration. Nevertheless, an obvious difference between the two neuron types is the uniglomerular innervations of mALT PNs versus the multiglomerular AL innervations of mlALT PNs. It might be that PNs in the mlALT informs downstream target neurons about the overall constellation of co-active AL glomeruli, and thus the general “odor image” of the environment, as realized by its multiglomerular dendritic branches. In contrast, the uniglomerular PNs in the mALT might serve to fine-tune the activity of a downstream LH neuron, possibly adjusting its activity according to the presence of a more evolutionary relevant chemical compound in the vicinity of the animal, linked to specific glomeruli.

The presence of GABAergic PNs in the mlALT has been reported for several insect species, including *H. virescens,* suggesting that neurons in this tract inhibit the downstream lateral horn neurons (LHN) (Berg et al., 2009). PNs of the mALT, on the other hand, are shown to be cholinergic (Wang et al., 2014). Such a dichotomy might allow for several possible coding paradigms at the AL-LH junction. For instance, if the two tracts originate from a similar configuration of AL

glomeruli, the excitatory influence of PNs confined to the mALT might be only brief on the LHNs, as a rapidly succeeding inhibition elicited by the mlALT input may halt their activity. Such an excitation-inhibition information transfer duality might be necessary for the rapid processing of olfactory information in the fluctuating, noisy odor environment presented to insects. A gain in speed of processing has, for instance, been used as an argument for a similar kind of duality realized in the ON and OFF ganglion cells in the visual system of mammals (Kandel, 2013).

In the AL network of *D. melanogaster,* Wang et al. (2014) found that mlALT PNs receive input from both ORNs and PNs of the mALT. Additionally, the GABAergic mlALT neurons were found to form electrical gap junctions with other AL neurons. This latter finding may explain why a mALT neuron was simultaneously stained in the preparation (p2) displaying mlALT PNs in this thesis.

4.1.2 | *Bilateral projection neuron in the dmALT*

A single bilateral PN passing in the dorsomedial antennal-lobe tract was stained in a male of the species *H. armigera* (p3). While the measured responses of this neuron were not significant, visual examination exposed alterations in the firing patterns. As demonstrated in figure 14, a spike pattern looking like a complex response occurred to stimulation with B12. Few previous studies have reported about dmALT neurons, probably because these neurons are scarce in number. In the moth species *M. sexta*, it has been estimated that the dmALT consist of only 16 fibers in both males and females (Homberg et al., 1988). In the silkmoth *B. mori*, only one dmALT neuron has been found so far, displaying a unilateral innervation pattern (Namiki and Kanzaki, 2011). Three dmALT neurons have been previously described in *H. virescens*, of which two incompletely stained neurons showed bilateral innervations (Ro et al., 2007). However, no data exists for *H. armigera*. Except for displaying multiglomerular innervations in the AL, one of the dmALT PNs presented by Ro et al. (2007) had similar morphological characteristics to the dmALT neuron shown in the present study.

Because the estimated number of dmALT neurons is far less than the number of glomeruli, and a substantial proportion of the dmALT PNs seems to be uniglomerular, one can speculate about the role of the target glomeruli being innervated by this category of projections neurons. So far, it has not been possible to map the glomeruli innervated by uniglomerular dmALT neurons because the number of registered neurons are still so few. Anyway, the identification of one bilateral dmALT neuron, as demonstrated in the study presented here, supports previous reports which imply the importance of this tract in processes including bilateral integration of olfactory information (Ro et al., 2007). Recently, however, mass-staining has shown a tract of about 50 neurons extending from the AL to the contralateral LH, which if conveying odor-responsive neurons may also aid bilateral processing (Kjos, 2016).

The stained dmALT neuron in the present study displays innervations in both the posterior and anterior region of the LH. Previous studies of several insect species have revealed that these two comparable LH subregions receive input from PNs conveying information about distinct odor categories (Jefferis et al., 2007, Roussel et al., 2014, Zhao et al., 2014). Zhao et al. (2014) showed that the medial-tract PNs originating from the MGC and the ordinary glomeruli in the AL, target the anterior and posterior regions of the LH, respectively. If the anatomical segregation in the LH is functionally relevant for olfactory processing in this higher-order area, the information conveyed along the dmALT PN might be of importance for both pheromone and plant odor processing, because of its innervation to both subregions. However, an anatomical segregation does not directly imply distinctions concerning a functional role.

4.1.3 | *Input neuron from the optic lobula plate*

A single stained neuron was found to densely innervate the optic lobula plate. In addition, branches of this neuron were seen in the ventromedial neuropils and both the ipsi- and contralateral LH. Because the neuronal recording obtained in this preparation showed responses to both a light source directed toward the insect and antennal stimulation with odors, it is likely that the branches in the LH ipsilateral to the lobula plate innervations are dendritic. The location of the cell body in the ipsilateral hemisphere of the innervations in the lobula plate, suggest this region to be dendritic. In this case, the neuron seems to integrate both visual and olfactory input, and project this information to the contralateral hemisphere.

Interestingly, in previous studies of *D. melanogaster*, the lateral protocerebrum is found to contain optical glomeruli (OPG) that share organizational similarities with the olfactory glomeruli of the AL (Strausfeld et al., 2007). These OPGs, located beneath the LH, receive input from both the lobula and lobula plate (Douglass and Strausfeld, 1998). Local interneurons connecting these OPGs are found to show spiking activity in the absence of visual stimuli, and their dendritic branches into the LH are suggested to convey information from other sensory modalities, like olfaction (Strausfeld et al., 2007). Similar to the findings of this thesis, such an arrangement proves the interconnection between the olfactory and visual modalities in this higher-order processing area.

It was noticed that neurons in the LH that displayed responses to a light stimulus, but not to odors, maintained a more robust activity during intracellular recording, reflected in spike amplitude and recording stability. Moreover, the fact that two of the totally five successfully stained preparations included neurons responding to both odor and light stimulus, may indicate that neurons carrying visual information are larger in diameter. Thus, these neurons may therefor be easier to penetrate and stain, compared to higher-order neurons carrying purely olfactory information.

4.1.4 | *Protocerebral interneuron*

A weakly stained protocerebral interneuron innervating the superior protocerebrum and the LH could be seen in p4. Generally, interneurons serve numerous functions, both in synchronizing neuronal activity, and modulating and maintaining network phenomena like oscillations (Lei et al., 2002, Laurent, 2002). For example, it has been suggested that LH interneurons create the sparse spiking seen in the mushroom body Kenyon cells (KCs). As excitatory input from PNs elicits a response in KCs, the KC responses will quickly be shut down by inhibitory input from LH interneurons, which also are driven by the excitatory PN input (Laurent, 2002). The protocerebral interneuron presented in this thesis was most likely stained by dye leakage across electrical gap junctions. Because of the deformed brain in p4, it is not possible to determine the precise target regions of this neuron. Interestingly, however, it seems to have electrical synapses with the large descending neuron R8.

4.2 | **Output from the lateral horn**

When orienting toward female moths, males perform an initial surge movement, followed by zig-zag casting, an olfactory orientation behaviour observed in several species, even humans (Carde and Willis, 2008, Porter et al., 2007). In insects, olfactory information eventually reaches the motoric centers of the ventral nerve cord via descending interneurons originating in the lateral accessory lobe (LAL). An identified sensory-motor circuit for pheromone processing in the moth species *B. mori*, as described by Namiki et al. (2014), suggests that the superior-medial protocerebrum is a relay between the so called delta-region of the inferior-lateral protocerebrum (ΔILPC) and the LAL in a pheromone-circuit. Thus, a separate pathway conveys pheromone signals from input to output, including the macroglomerular complex, a sexually dimorphic collection of pheromone responsive glomeruli in the AL, the ΔILPC in the LH, the superior medial protocerebrum, the LAL, and finally descending neurons initiating motor output (Namiki et al., 2014). A similar, but shorter, pheromone pathway was found in *D. melanogaster*, where input to the LH was confined to four clusters of neurons. Third-order LH neurons were found to project further to a triangular neuropil in the lateral protocerebrum and a distinct tract within the superior medial protocerebrum, and synapse onto descending neurons in these two areas (Ruta et al., 2010). For the processing of plant odorants, a putative circuit have been suggested, which includes a greater area of the superior and lateral protocerebrum, as well as the mushroom body lobes (Lofaldli et al., 2010).

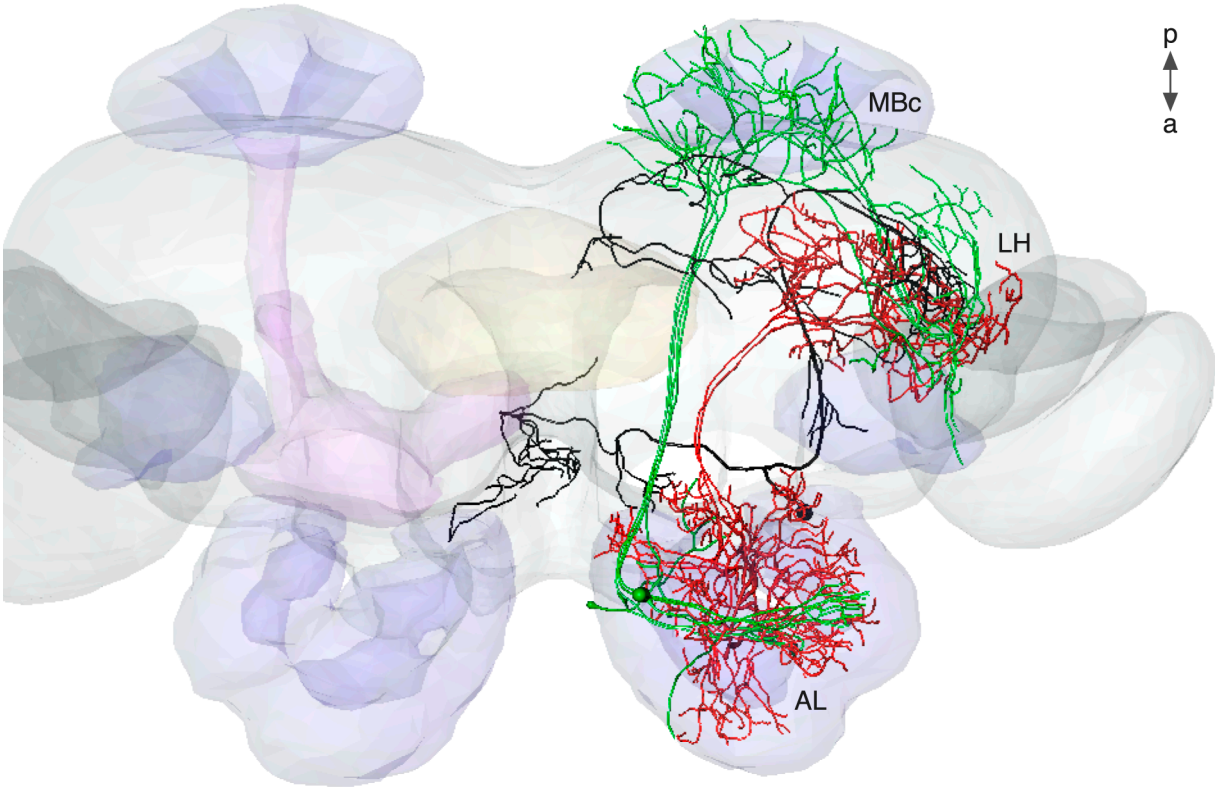

Figure 20 | **Schematic showing the overlap of antennal-lobe projection neurons (PNs) and protocerebral descending neuron in the lateral horn (LH)**. Dorsal view: The PNs constrained to medial- and medio-lateral antennal lobe tract (mALT and mlALT), from preparation 1 and 2, are coloured green and red, respectively. The protocerebral descending neuron stained in preparation 4 is coloured black. An overlap between all these neurons can be seen in the LH. The right peduncle and mushroom body lobes are hidden for a better visualization. *MBc = Mushroom body calyx.*

4.2.1 | *Protocerebral descending neuron*

A large descending neuron, innervating a relatively wide spectrum of the protocerebrum, including the LH, was stained in p4. Its axon was found to run along the mushroom body peduncle before projecting ventrally down the protocerebrum, crossing into the contralateral hemisphere and innervating the SEG. On its way, the neuron ran through the LAL, however no clear innervations could be seen. The direct projection to the SEG, circumventing the LAL, implies that this neuron serves a direct route between second-order olfactory neurons and pre-motoric output, running in parallel to the previously described pheromone route innervating the LAL. Notably, the innervating region of the descending neuron in the LH seems to overlap with the terminal region of neurons in the medial and mediolateral ALT, stained in p1 and p2 (fig 20).

The physiological data obtained from the descending neuron demonstrated responses to a light stimulus, as well as to odor stimulation to the antennae. Significant odor responses were obtained for both sunflower and the ideal pheromone mixture, whereas neither B12 nor linalool elicited

any response. The odor responses did not outlast the stimulation period in any trial, but typically showed a persistent response during the stimulation. Due to the descending neuron's direct projection to the SEG, its widespread innervation in the protocerebrum, and its stimulus-tied response duration, it might be that such a neuron acts as a modulator for motoric output. By eliciting a small excitatory increase in firing rate in the presence of the natural plant and/or pheromone mixture, the neuron might serve to increase the likelihood of firing in downstream pre-motoric neurons. However, because the stimulus was only presented at a fixed 400 ms window, it is not possible to say how this neuron would react to longer-lasting stimulations.

4.3 | **Olfactory processing in the lateral horn**

Understanding olfactory processing is a challenging enterprise. Firstly, insect olfaction is not a passive act, but rather a task in which flicking movements of the antennae are precisely coordinated to better detect concentrations and directions of the encountered odor plumes (Hillier and Vickers, 2004). Secondly, one must realise that the responses observed in central olfactory neurons is not the end point of some olfactory processing, except perhaps at the motor-neuron junction. Rather, the precise spike-timing reflects a current computation and transformation of the detected signal, which at any level of processing may be distributed across a larger population of interconnected neurons.

The present study has shown that individual neurons in the LH are most responsive to naturally occurring odor mixtures. However, due to the lack of morphological data for most of the tested neurons, these recordings may include both second- and third-order olfactory neurons, as well as interneurons. One observation made was that intracellular contact with neurons, and the likelihood of responses, was easier to obtain in the more medial region of the LH than at the lateral rim of the protocerebrum.

4.3.1 | *General responses*

A high spontaneous activity could be seen in neurons recorded from the LH, typically ranging from 20-80 HZ. In several neurons, it was also observed a shift in spontaneous activity throughout the experiment. It is not possible to tell whether this is due to intrinsic alterations in the firing of the neuron owing to odor stimulation, or as a result of movement of the microelectrode used for recording.

In general, the present study shows that recorded neurons in the LH of the two related *Heliothinae* moths are most responsive to the naturally occurring plant volatile mixture emitted by sunflower, rather than single plant components. This finding is in contrast to the responses reported in peripheral olfactory sensory neurons in *Heliothinae* moths, which is found to respond almost

exclusively to single substances, with only weak responses to highly similar compounds (Rostelien et al., 2005). We thereby see that higher-order neurons require the presence of a mixture of odor compounds in order to show a response. Interestingly, the primary pheromone component elicited a response in a greater percent of tested neurons than did the ideal pheromone mixture. It might be that single component pheromone information is kept separated in the LH, differing from the findings of plant odor components as described above. However, because the pure pheromone components were tested in such a limited number of preparations, this might be simply due to chance.

The maximum firing rate differed between neurons, but were generally found to be consistent across odor responses within one neuron. The majority of responses were found to be excitatory, while only one neuron responded with inhibition to antennal odor stimulation. Some neurons also exhibited complex responses, which included intermingled excitatory and inhibitory phases. Complex activity can be explained in light of attractor network dynamics, in which the constellation of co-active PNs evolve toward a stable pattern of activity (explained in section 1.2.5). During this process, some PNs are excited or inhibited at different times owing to the network activity in the AL. As a result, fluctuating (complex) activity in some PNs and third-order neurons might occur.

In a previous study by Lofaldli et al. (2010), performing similar recordings from the LH of *H. virescens* females, 96% of 50 tested neurons showed response to the plant odor component mixture blend 12 (B12), in contrast to only 55% of the 21 responding neurons in this thesis. This might be purely accidental, as the number of recordings in the present study are limited. The same is true for linalool and germacrene D, which both elicited a response in 82% of the tested neurons in the study by Lofaldli et al. (2010), while 31% and 0% of the 21 neurons in the present study showed a significant response to linalool and germacrene D, respectively. In the present study, the neuron recordings were obtained by lowering the microelectrode into the LH from a dorsal position. Lofaldli et al. (2010) however, used a different orientation of the animal, entering the LH from a sagittal position. This might have resulted in contact with fibre bundles being connected with different subsets of LH neurons, or even antennal-lobe projection neurons.

Behavioural studies combining gas chromatography linked with mass spectrometry have revealed that attractant flowers visited by the moth species *M. sexta* share a common sensory signal, namely methyl benzoate (Riffell et al., 2013). A similar key odor might also be present for flowers visited by *Heliothinae* moths. Previous work with *H. virescens*, investigating the odor tuning of sensory neurons in the antenna, reported that 65 out of 80 recorded sensory neurons was highly specialized for detecting the sesquiterpene germacrene D (Rostelien et al., 2000). Similar findings are also reported for *H. armigera* (Stranden et al., 2002). These findings might

explaining the great amount of responses in the LH to this particular substance as shown by Lofaldli et al. (2010), however opposite to the findings presented here. In fact, host tobacco plants dispensing germacrene D were found to be more attractive for mated female *H. virescens* in a wind-tunnel study, compared to tobacco plants without germacrene D (Mozuraitis et al., 2002).

The relatively broad tuning observed in neuronal recordings obtained in the present study, except for the low amount of responses to the single plant components, is in agreement with the findings of Lofaldli et al. (2010). In *D. melanogaster*, it has been shown that LH neurons receive input from sparse and stereotyped combinations of AL glomeruli being co-activated by odors (Fisek and Wilson, 2014). The same study also showed that while one class of LH neurons were broadly tuned, summing the input of several glomeruli, another class of LH neurons were narrowly tuned, receiving input from a small number of glomeruli. Whether such a dichotomy also exists for LH neurons in *Heliothinae* moths, is an open question requiring further investigations.

Since each odor component was diluted in hexane, pure hexane was used as control. Previous calcium-imaging measurements from *H. virescens* have revealed minor responses to the control stimulus, consisting of hexane, in the shape of activation patterns in one or two glomeruli of the AL, attributed either to the hexane component or a mechanosensory input (Skiri et al., 2004). Surprisingly, almost half of the 21 neurons tested in the present study responded with either a complex or excitatory response to the pure hexane. Because both sunflower and hexane were tested in every preparation, there is a risk of a contamination of the control glass cartridge. However, in the work by Lofaldli et al. (2010), 32% of the odor-responsive neurons also responded to the control, which in their case was a clean filter paper with no hexane. It might very well be, since test substances are presented in a pseudorandom fashion, that associative learning takes place. A previously presented odor combined with the air puff might have established a new response to either just the pure air or pure hexane in a subsequent stimulation. Furthermore, one could only speculate whether these responses are attributed to the filter paper itself, or remnants of wood fibres in the filter papers from the process of making them, or some expectation or learning mechanism as described above. Nevertheless, except for N20, all neurons responding to pure hexane demonstrated odor-specific responses by responding not to every tested odorant, but to selected compounds. A mere mechano-evoked response could therefore be disregarded. Nor the response observed in N20 was unambiguously mechanosensory, since the response durations differed for the tested components.

4.3.2 | *Female autodetection of pheromones*

Interestingly, the only female preparation used in the study was also the only insect that showed responses to pheromones exclusively. While behavioural studies have shown that male-produced sex-pheromones might be important for attracting females, the females of several moth species are considered to be anosmic of their own pheromones (Hillier and Vickers, 2004, Stelinski et al., 2006). However, electroantennogram recordings and behavioural analysis have shown autodetection of pheromones in females of several moth species (Stelinski et al., 2006, Schneider et al., 1998, Weissling and Knight, 1996). For example, in the codling moth *Cydia pomonella*, presence of the primary pheromone component codlemone in the air was found to elicit a significantly higher calling in females, compared to females calls in an environment free of codlemone (Weissling and Knight, 1996). The functional role of autodetection makes sense as it would be an advantage to be aware of competing females in the vicinity. In fact, in a choice test, females were found to deposit more eggs on uncontaminated wax paper, than on paper contaminated with codlemone (Weissling and Knight, 1996). While this thesis did not systematically investigate responses in females, the finding hints to a mechanism of autodetection. In fact, while the four glomeruli comprising the macroglomerular complex is present in males only, a similar assembly of two enlarged glomeruli is found to be present at a corresponding location in females (Berg et al., 2002).

4.3.3 | *Long lasting excitation in protocerebral neurons*

Both neuron N3 and N18 showed long response durations to sunflower, outlasting the stimulus period with at least four seconds (fig 9). N18 also showed a relatively long response duration to the ideal pheromone blend, yet not as long as the response elicited by sunflower. In addition, N18 responded with a similarly long-lasting excitation to an interspecific signal, B12, and the control. However, the response duration and latency of onset differed for the stimuli. This was seen most notably for the control, where an onset latency of 1000 ms was followed by 1000 ms excitation, compared with the response of sunflower which displayed an immediate response onset, followed by 4500 ms excitation. Also, N18 was found to be the neuron with the largest maximum firing rate after stimulus onset, at about 300 HZ. In *H. virescens*, long lasting excitation (LLE) responses have previously been found during stimulation with a blend of ten relevant plant odor components, lasting between 1000 to 2500 ms (Lofaldli et al., 2012). These latter responses, however briefer, resemble the responses elicited by sunflower in the present study. A similar LLE, lasting for about 1000 to 2000 ms, has been reported in protocerebral neurons in the turnip moth *Agrotis segetum* during exposure to the pheromone blend (Lei et al., 2001). In addition, investigations in both *M. sexta* and *B. mori* have revealed LLE in bilateral neurons connecting the LAL and the ventro-lateral protocerebrum (VLPC) in the two hemispheres. In fact, in these species, pheromone-evoked

responses as long as 30 seconds have been reported (Kanzaki et al., 1991, Kanzaki and Shibuya, 1992). These LLE responses were observed more often during testing with the pheromone blend than when delivering the individual pheromone components. Such neuron responses were however rare. In relation to pheromone processing, the LAL-VLPC can be considered a functional unit, suggested to be involved in a flip-flop system, where reciprocal inhibition and excitation by bilateral neurons connecting the LAL-VLPC units in both hemispheres display long-lasting activity (Iwano et al., 2010). This in turn controls the zig-zag behaviour observed in male moths in response to pheromones produced by the female (Iwano et al., 2010).

While such a flip-flop system has not been described for the plant odor system in insects, it is reasonable to assume that a similar arrangement may exist to enable plant localization. This system most likely also includes input from the visual system as well, as flight behaviour toward plants are shown to be modulated by the presence of multimodal information (Balkenius and Dacke, 2010).

Because volatile odor components released by plants extend into the environment as odor plumes with interspersed empty regions, the scent of a plant is not continuously present, but rather exists as discrete odor packets in a noisy odor environment (Koehl, 2006). LLE neurons might therefor also serve to motivate searching behaviour, or function as a short-term memory for the presence of a plant in the close environment. Such a neural short-term memory mechanism may be achieved through a network exhibiting recurrent connectivity, as seen with neurons that display selective delay activity in the cerebral cortex of mammals (Amit and Mongillo, 2003).

Interestingly, recording N3 showed a trial-dependent response duration, in which the first trial resulted in a LLE of almost 5000 ms, while the excitatory response to the second stimulus trial lasted only about 600 ms. A subsequent repeat of two trials 200 seconds later, revealed an identical response pattern (fig 9). The neuron looks thereby to adapt to odor presentation after a single trial, but is then reset after an intermission period.

Because of the lacking morphology on the LLE responsive neurons N3 and N18, any further interpretation of the two neurons' function is not possible.

4.3.4 | *Multimodal integration of visual and olfactory information*

In the dim light of the night, insects, like the nocturnal *Heliothinae* moths, demonstrate a diverse nature of visual practices to navigate their environment. These include both colour night vision, and the remarkable feat of using polarized light from the moon for orientation (Kelber et al., 2002, Dacke et al., 2003). Sensory information from several modalities has previously been observed to innervate the insect lateral horn, including visual, olfactory and gustatory signals (Gupta and Stopfer, 2012, Homberg et al., 1988, Kvello et al., 2009). In the present study, 4 out of 21 odor-

responding neurons also responded to a light stimulus (19%), of which two were successfully stained. In fact, most of the neurons encountered in the LH during the experiments responded only to visual stimuli, but because these neurons did not respond olfactory stimulation of the antenna, they have not been included in the thesis. Three of the four multimodal neurons presented in this thesis were moderately inhibited by light and showed a quick burst in activity when the light was switched off. The opposite was true for the one remaining neuron; here light onset induced a transient burst in activity. Also, all multimodal neurons showed a flat ISI histogram shape. The network-level functionality of this multimodal integration in the LH requires further investigation. However, behavioural studies have reported that integration of visual, olfactory and mechanosensory inputs is important for in-flight odor tracking in both *D. melanogaster* and the hawkmoth *M. sexta* (Duistermars and Frye, 2009, Balkenius and Dacke, 2010). It may be that the presence of light inhibits plant or female searching behaviour in night-active moth species like *Heliothinae*. In this way, day-time light would serve as a powerful modulator (inhibitor) of olfactory-driven behaviour.

4.4 | **Methodological considerations**

In previous studies investigating the morphology of AL PNs in moths, staining have been applied directly into the dendrites or somata in the AL. Staining from the LH brings the advantage of leaving dendritic AL innervations of the PNs perfectly intact, as no damage with a penetrating electrode is done.

While antennal stimulation with single plant components such as linalool allows for a valuable understanding of early olfactory processing, such pure components are unlikely to be encountered by an insect in the wild. Stimuli made from realistic plant odor mixtures such as sunflower, might therefore be necessary to include as test stimuli in order to obtained responses from neurons at higher-level regions of the olfactory system, as done in this thesis.

4.4.1 | *Limitations with intracellular recording and spike analysis*

The whole-cell sharp electrode recording method used in this study, in contrast to the patch-clamp technique, makes a less tight seal with the recorded neuron. Because intracellular recording disruptively penetrates the neural tissue, it may alter the ion concentration across the neuron membrane. Eventually, this may affect the activity of the recorded cell or even the function of its connected network. In addition, owing to the unstable nature of intracellular recording, particularly from the small brain of *Heliothinae* moths, it was not possible to test all odorants across all neurons. This of course limits the results of analysis. Also, because of the limited number

of preparations showing a successful staining, it was not possible to find correlations between morphological properties and spontaneous activity reflected by the inter-spike intervals.

The use of algorithmic approaches to determine responses can be problematic when a large variation in response duration and strength is seen. The use of two response classifiers, one based on a dynamic response window estimation, and one based on a rigid 400 ms response window, were best able to reflect the subjectively interpreted response-physiology of the neurons. It should be noted that due to the complex undertaking of the neural circuits related to sensory systems, even responses considered statistically insignificant is most likely biologically relevant to the insect. The specific timing of a single spike, in relation to synchronized activity in a population of neurons as measured by their associated local field potential, has indeed been shown to play an important role in neuronal signalling (Wehr and Laurent, 1996). In fact, as long as the timing of spikes are synchronized among a large population of neurons targeting the same down-stream neuron, the firing rate of the individual neurons may not need to increase at all, but merely be adjusted to fit the precise, synchronous spike timing of the population.

4.4.2 | *Further studies*

Once entering the nervous system, sensory signals are distributed across populations of neurons, where the information is transformed and allocated. To further understand LH function, future studies should complement intracellular recording by investigating the population responses in LH neurons, by means of extracellular recording or calcium-imaging techniques. Development of genetic tools to unveil circuit functions in moths would aid such an investigation, but so far this progress has been lagging behind that of *D. melanogaster*. However, recent advances in the field may open up to new possibilities, like development of a GAL4 line for visualization and manipulation of neurons expressing the BmOR1 receptor, tuned to detect the primary pheromone component bombykol in *B. mori* (Kiya et al., 2014). A systematic investigation of pheromone component integration and/or the integration of signals originating from pheromone and non-pheromone components in higher order areas is necessary to fully understand these circuits. Finally, further investigation of pheromone autodetection in females would be interesting, as this thesis have shown neurophysiological responses to both the pheromone mixture and individual components through LH recording in a female.

5 | Conclusions

- Intracellular iontophoretic staining performed from the lateral horn (LH), demonstrated the suitability of this technical approach for characterizing antennal-lobe projection neurons by successful labelling of seven such neurons; four in the medial antennal-lobe tract (mALT), two in the mediolateral ALT (mlALT), and one previously undescribed bilateral neuron in the dorsomedial ALT (dmALT).
- The projection neurons confined to the mALT and mlALT were found to overlap in the LH.
- The successfully labelled preparations demonstrate the presence of individual neurons integrating information about light and odor. Two multimodal neurons innervating the lateral horn were stained; one protocerebral descending neuron and one bilateral neuron extending from the ipsilateral optic lobula plate.
- Antennal stimulation with biologically relevant odors revealed that neurons in the LH are most responsive to natural odor mixtures, like the headspace sample from sunflower and the ideal pheromone mixture emitted by the female of the same species.
- Long lasting excitation was observed in two neuron recordings in response to antennal stimulation with sunflower, including responses that outlasted the stimulus period by 4 seconds.
- A substantial amount of neurons in the lateral horn were found to integrate olfactory and visual stimuli, as 19% of odor-responding neurons also responded to a light stimulus.
- Responses to both the ideal pheromone mixture and its individual components were observed when recording from a female of the species *Helicoverpa armigera*, suggesting that females of this species is capable of pheromone autodetection.

Abbreviations

ACC	Anterior cell cluster
AL	Antennal-lobe
ALT	Antennal-lobe tract
AOT	Anterior optic tubercle
CB	Central body
dALT	Dorsal antennal-lobe tract
ΔILPC	Delta region of the inferior lateral protocerebrum
dmALT	Dorsomedial antennal-lobe tract
GABA	γ-aminobutyric acid
ISI	Inter-spike interval
KC	Kenyon cell
lALT	lateral antennal-lobe tract
LCC	Lateral cell cluster
LH	Lateral horn
LHN	Lateral horn neurons
LN	Local interneurons
LOp	Lobula plate
LP	Lateral protocerebrum
mALT	Medial antennal-lobe tract
MBc	Mushroom body calyx
MCC	Medial cell cluster
MDS	Mean deviation from spontaneous activity
MGC	Macroglomerular complex
mlALT	Mediolateral antennal-lobe tract
N1-21	Neuron 1 to 21
OB	Olfactory bulb
OR	Olfactory receptor
OSN	Olfactory sensory neuron
P1-P5	Preparation 1 to 5
R1-10	Reconstruction 1 to 10
SBA	Standard brain atlas
SEG	Subesophageal ganglion
SMP	Superior-medial protocerebrum
tALT	Transverse antennal-lobe tract
VLPC	Ventrolateral protocerebrum

References

ADRIAN, E. D., BRONK, D. W. & PHILLIPS, G. 1932. Discharges in mammalian sympathetic nerves. *J Physiol,* 74**,** 115-33.

AMIT, D. J. & MONGILLO, G. 2003. Selective delay activity in the cortex: phenomena and interpretation. *Cereb Cortex,* 13**,** 1139-50.

ANDERSSON, M. N., LOFSTEDT, C. & NEWCOMB, R. D. 2015. Insect olfaction and the evolution of receptor tuning. *Frontiers in Ecology and Evolution,* 3**,** 14.

AVERBECK, B. B., LATHAM, P. E. & POUGET, A. 2006. Neural correlations, population coding and computation. *Nat Rev Neurosci,* 7**,** 358-66.

BALKENIUS, A. & DACKE, M. 2010. Flight behaviour of the hawkmoth Manduca sexta towards unimodal and multimodal targets. *J Exp Biol,* 213**,** 3741-7.

BATESON, M., DESIRE, S., GARTSIDE, S. E. & WRIGHT, G. A. 2011. Agitated honeybees exhibit pessimistic cognitive biases. *Curr Biol,* 21**,** 1070-3.

BEKKERS, J. M. & SUZUKI, N. 2013. Neurons and circuits for odor processing in the piriform cortex. *Trends Neurosci,* 36**,** 429-38.

BERG, B., ZHAO, X.-C. & WANG, G. 2014. Processing of Pheromone Information in Related Species of Heliothine Moths. *Insects,* 5**,** 742-761.

BERG, B. G., GALIZIA, C. G., BRANDT, R. & MUSTAPARTA, H. 2002. Digital atlases of the antennal lobe in two species of tobacco budworm moths, the Oriental Helicoverpa assulta (male) and the American Heliothis virescens (male and female). *J Comp Neurol,* 446**,** 123-34.

BERG, B. G., SCHACHTNER, J. & HOMBERG, U. 2009. Gamma-aminobutyric acid immunostaining in the antennal lobe of the moth Heliothis virescens and its colocalization with neuropeptides. *Cell Tissue Res,* 335**,** 593-605.

BUZSÁKI, G. 2006. *Rhythms of the brain,* Oxford ; New York, Oxford University Press.

CARDE, R. T. & WILLIS, M. A. 2008. Navigational strategies used by insects to find distant, wind-borne sources of odor. *J Chem Ecol,* 34**,** 854-66.

CHAPMAN, A. D. 2009. *Numbers of living species in Australia and the world*, Canberra: Australian Biological Resource Study.

CHRISTENSEN, T. A., WALDROP, B. R., HARROW, I. D. & HILDEBRAND, J. G. 1993. Local interneurons and information processing in the olfactory glomeruli of the moth Manduca sexta. *J Comp Physiol A,* 173**,** 385-99.

COUTO, A., ALENIUS, M. & DICKSON, B. J. 2005. Molecular, anatomical, and functional organization of the Drosophila olfactory system. *Curr Biol,* 15**,** 1535-47.

DACKE, M., NILSSON, D. E., SCHOLTZ, C. H., BYRNE, M. & WARRANT, E. J. 2003. Animal behaviour: insect orientation to polarized moonlight. *Nature,* 424**,** 33.

DAYAN, P. & ABBOTT, L. F. 2001. *Theoretical neuroscience : computational and mathematical modeling of neural systems,* Cambridge, Mass., Massachusetts Institute of Technology Press.

DE BELLE, J. S. & HEISENBERG, M. 1994. Associative odor learning in Drosophila abolished by chemical ablation of mushroom bodies. *Science,* 263**,** 692-5.

DOUGLASS, J. K. & STRAUSFELD, N. J. 1998. Functionally and anatomically segregated visual pathways in the lobula complex of a calliphorid fly. *J Comp Neurol,* 396**,** 84-104.

DUISTERMARS, B. & FRYE, M. A. 2009. Multisensory integration for odor tracking by flying Drosophila. *Commun Integr Biol,* 3**,** 60-63.

DUISTERMARS, B. J. & FRYE, M. A. 2010. Multisensory integration for odor tracking by flying Drosophila: Behavior, circuits and speculation. *Commun Integr Biol,* 3**,** 60-3.

EISEMANN, C. H., JORGENSEN, W. K., MERRITT, D. J., RICE, M. J., CRIBB, B. W., WEBB, P. D. & ZALUCKI, M. P. 1984. Do insects feel pain? A biological view. *Cellular and Molecular Life Sciences,* 40**,** 164-167.

FISEK, M. & WILSON, R. I. 2014. Stereotyped connectivity and computations in higher-order olfactory neurons. *Nat Neurosci,* 17**,** 280-8.

FITT, G. P. 1989. The Ecology of Heliothis Species in Relation to Agroecosystems. *Annual Review of Entomology,* 34**,** 17-52.

FORNITO, A., ZALESKY, A. & BREAKSPEAR, M. 2015. The connectomics of brain disorders. *Nat Rev Neurosci,* 16**,** 159-72.

FRIEDRICH, R. W., HABERMANN, C. J. & LAURENT, G. 2004. Multiplexing using synchrony in the zebrafish olfactory bulb. *Nat Neurosci,* 7**,** 862-71.

FRIEDRICH, R. W. & WIECHERT, M. T. 2014. Neuronal circuits and computations: pattern decorrelation in the olfactory bulb. *FEBS Lett,* 588**,** 2504-13.

GALAN, R. F., SACHSE, S., GALIZIA, C. G. & HERZ, A. V. M. 2004. Odor-driven attractor dynamics in the antennal lobe allow for simple and rapid olfactory pattern classification. *Neural Computation,* 16**,** 999-1012.

GALIZIA, C. G. & LLEDO, P.-M. 2013. *Neurosciences : from molecule to behavior : a university textbook,* Heidelberg ; New York, Springer Spektrum.

GALIZIA, C. G. & ROSSLER, W. 2010. Parallel olfactory systems in insects: anatomy and function. *Annu Rev Entomol,* 55**,** 399-420.

GALIZIA, C. G., SACHSE, S. & MUSTAPARTA, H. 2000. Calcium responses to pheromones and plant odours in the antennal lobe of the male and female moth Heliothis virescens. *J Comp Physiol A,* 186**,** 1049-63.

GOTTFRIED, J. A. 2010. Central mechanisms of odour object perception. *Nat Rev Neurosci,* 11**,** 628-41.

GUPTA, N. & STOPFER, M. 2012. Functional analysis of a higher olfactory center, the lateral horn. *J Neurosci,* 32**,** 8138-48.

HANSSON, B. S. 1999. *Insect olfaction,* Berlin ; New York, Springer.

HILLIER, N. K. & VICKERS, N. J. 2004. The role of heliothine hairpencil compounds in female Heliothis virescens (Lepidoptera: Noctuidae) behavior and mate acceptance. *Chem Senses,* 29**,** 499-511.

HOMBERG, U., MONTAGUE, R. A. & HILDEBRAND, J. G. 1988. Anatomy of antenno-cerebral pathways in the brain of the sphinx moth Manduca sexta. *Cell Tissue Res,* 254**,** 255-81.

HONEGGER, K. S., CAMPBELL, R. A. & TURNER, G. C. 2011. Cellular-resolution population imaging reveals robust sparse coding in the Drosophila mushroom body. *J Neurosci,* 31**,** 11772-85.

HØYDAL, Ø. 2012. *Central Processing of Plant Odor Mixtures and Single Odorants in the Moth Heliothis Virescens.* Master's thesis in Biology, Norwegian University of Sciences and Technology.

IAN, E., BERG, A., LILLEVOLL, S. C. & BERG, B. G. 2016. Antennal-lobe tracts in the noctuid moth, Heliothis virescens: new anatomical findings. Manuscript submitted for publication. *Cell Tissue Res*.

ITO, I., ONG, R. C., RAMAN, B. & STOPFER, M. 2008. Sparse odor representation and olfactory learning. *Nat Neurosci,* 11**,** 1177-84.

ITO, K., SHINOMIYA, K., ITO, M., ARMSTRONG, J. D., BOYAN, G., HARTENSTEIN, V., HARZSCH, S., HEISENBERG, M., HOMBERG, U., JENETT, A., KESHISHIAN, H., RESTIFO, L. L., ROSSLER, W., SIMPSON, J. H., STRAUSFELD, N. J., STRAUSS, R., VOSSHALL, L. B. & INSECT BRAIN NAME WORKING, G. 2014. A systematic nomenclature for the insect brain. *Neuron,* 81**,** 755-65.

IWANO, M., HILL, E. S., MORI, A., MISHIMA, T., MISHIMA, T., ITO, K. & KANZAKI, R. 2010. Neurons associated with the flip-flop activity in the lateral accessory lobe and ventral protocerebrum of the silkworm moth brain. *J Comp Neurol,* 518**,** 366-88.

JEFFERIS, G. S., POTTER, C. J., CHAN, A. M., MARIN, E. C., ROHLFING, T., MAURER, C. R., JR. & LUO, L. 2007. Comprehensive maps of Drosophila higher olfactory centers: spatially segregated fruit and pheromone representation. *Cell,* 128**,** 1187-203.

JORTNER, R. A. 2013. Neural coding in the olfactory system. *In:* QUIROGA, R. Q. & PANZERI, S. (eds.) *Principles of neural coding.* CRC Press.

KANDEL, E. R. 2013. *Principles of neural science,* New York, McGraw-Hill.

KANZAKI, R., ARBAS, E. A. & HILDEBRAND, J. G. 1991. Physiology and morphology of protocerebral olfactory neurons in the male moth Manduca sexta. *J Comp Physiol A,* 168**,** 281-98.

KANZAKI, R. & SHIBUYA, T. 1992. Long-lasting excitation of protocerebral bilateral neurons in the pheromone-processing pathways of the male moth Bombyx mori. *Brain Res,* 587**,** 211-5.

KAUPP, U. B. 2010. Olfactory signalling in vertebrates and insects: differences and commonalities. *Nat Rev Neurosci,* 11**,** 188-200.

KELBER, A., BALKENIUS, A. & WARRANT, E. J. 2002. Scotopic colour vision in nocturnal hawkmoths. *Nature,* 419**,** 922-5.

KIYA, T., MORISHITA, K., UCHINO, K., IWAMI, M. & SEZUTSU, H. 2014. Establishment of tools for neurogenetic analysis of sexual behavior in the silkmoth, Bombyx mori. *PLoS One,* 9**,** e113156.

KJOS, I. C. 2016. *Mapping neural networks linked to a higher olfactory center in a model brain.* Master's thesis in Psychology, Norwegian University of Science and Technology.

KOEHL, M. A. 2006. The fluid mechanics of arthropod sniffing in turbulent odor plumes. *Chem Senses,* 31**,** 93-105.

KVELLO, P., LOFALDLI, B. B., RYBAK, J., MENZEL, R. & MUSTAPARTA, H. 2009. Digital, Three-dimensional Average Shaped Atlas of the Heliothis Virescens Brain with Integrated Gustatory and Olfactory Neurons. *Front Syst Neurosci,* 3**,** 14.

LAURENT, G. 2002. Olfactory network dynamics and the coding of multidimensional signals. *Nat Rev Neurosci,* 3**,** 884-95.

LEE, J. K. & STRAUSFELD, N. J. 1990. Structure, Distribution and Number of Surface Sensilla and Their Receptor-Cells on the Olfactory Appendage of the Male Moth Manduca-Sexta. *Journal of Neurocytology,* 19**,** 519-538.

LEI, H., ANTON, S. & HANSSON, B. S. 2001. Olfactory protocerebral pathways processing sex pheromone and plant odor information in the male moth Agrotis segetum. *J Comp Neurol,* 432**,** 356-70.

LEI, H., CHRISTENSEN, T. A. & HILDEBRAND, J. G. 2002. Local inhibition modulates odor-evoked synchronization of glomerulus-specific output neurons. *Nat Neurosci,* 5**,** 557-65.

LOFALDLI, B. B., KVELLO, P., KIRKERUD, N. & MUSTAPARTA, H. 2012. Activity in Neurons of a Putative Protocerebral Circuit Representing Information about a 10 Component Plant Odor Blend in Heliothis virescens. *Front Syst Neurosci,* 6**,** 64.

LOFALDLI, B. B., KVELLO, P. & MUSTAPARTA, H. 2010. Integration of the antennal lobe glomeruli and three projection neurons in the standard brain atlas of the moth heliothis virescens. *Front Syst Neurosci,* 4**,** 5.

MARTIN, J. P., BEYERLEIN, A., DACKS, A. M., REISENMAN, C. E., RIFFELL, J. A., LEI, H. & HILDEBRAND, J. G. 2011. The neurobiology of insect olfaction: sensory processing in a comparative context. *Prog Neurobiol,* 95**,** 427-47.

MATHEW, D., MARTELLI, C., KELLEY-SWIFT, E., BRUSALIS, C., GERSHOW, M., SAMUEL, A. D., EMONET, T. & CARLSON, J. R. 2013. Functional diversity among sensory receptors in a Drosophila olfactory circuit. *Proc Natl Acad Sci U S A,* 110**,** E2134-43.

MATSUMOTO, S. G. & HILDEBRAND, J. G. 1981. Olfactory Mechanisms in the Moth Manduca-Sexta - Response Characteristics and Morphology of Central Neurons in the Antennal Lobes. *Proceedings of the Royal Society Series B-Biological Sciences,* 213**,** 249-+.

MAZOR, O. & LAURENT, G. 2005. Transient dynamics versus fixed points in odor representations by locust antennal lobe projection neurons. *Neuron,* 48**,** 661-73.

MORI, K., NAGAO, H. & YOSHIHARA, Y. 1999. The olfactory bulb: coding and processing of odor molecule information. *Science,* 286**,** 711-5.

MOZURAITIS, R., STRANDEN, M., RAMIREZ, M. I., BORG-KARLSON, A. K. & MUSTAPARTA, H. 2002. (-)-Germacrene D increases attraction and oviposition by the tobacco budworm moth Heliothis virescens. *Chem Senses,* 27**,** 505-9.

NAMIKI, S., IWABUCHI, S., PANSOPHA KONO, P. & KANZAKI, R. 2014. Information flow through neural circuits for pheromone orientation. *Nat Commun,* 5**,** 5919.

NAMIKI, S. & KANZAKI, R. 2011. Heterogeneity in dendritic morphology of moth antennal lobe projection neurons. *J Comp Neurol,* 519**,** 3367-86.

NIELSEN, B. L., JEZIERSKI, T., BOLHUIS, J. E., AMO, L., ROSELL, F., OOSTINDJER, M., CHRISTENSEN, J. W., MCKEEGAN, D., WELLS, D. L. & HEPPER, P. 2015. Olfaction: An Overlooked Sensory Modality in Applied Ethology and Animal Welfare. *Front Vet Sci,* 2**,** 69.

PORTER, J., CRAVEN, B., KHAN, R. M., CHANG, S. J., KANG, I., JUDKEWITZ, B., VOLPE, J., SETTLES, G. & SOBEL, N. 2007. Mechanisms of scent-tracking in humans. *Nat Neurosci,* 10**,** 27-9.

PURVES, D. 2012. *Neuroscience,* Sunderland, Mass., Sinauer Associates.

RIFFELL, J. A., LEI, H., ABRELL, L. & HILDEBRAND, J. G. 2013. Neural basis of a pollinator's buffet: olfactory specialization and learning in Manduca sexta. *Science,* 339**,** 200-4.

RO, H., MULLER, D. & MUSTAPARTA, H. 2007. Anatomical organization of antennal lobe projection neurons in the moth Heliothis virescens. *J Comp Neurol,* 500**,** 658-75.

ROSTELIEN, T., BORG-KARLSON, A. K., FALDT, J., JACOBSSON, U. & MUSTAPARTA, H. 2000. The plant sesquiterpene germacrene D specifically activates a major type of antennal receptor neuron of the tobacco budworm moth Heliothis virescens. *Chem Senses,* 25**,** 141-8.

ROSTELIEN, T., STRANDEN, M., BORG-KARLSON, A. K. & MUSTAPARTA, H. 2005. Olfactory receptor neurons in two Heliothine moth species responding selectively to aliphatic green leaf volatiles, aromatic compounds, monoterpenes and sesquiterpenes of plant origin. *Chem Senses,* 30**,** 443-61.

ROUSSEL, E., CARCAUD, J., COMBE, M., GIURFA, M. & SANDOZ, J. C. 2014. Olfactory coding in the honeybee lateral horn. *Curr Biol,* 24**,** 561-7.

RUBIN, B. D. & KATZ, L. C. 1999. Optical imaging of odorant representations in the mammalian olfactory bulb. *Neuron,* 23**,** 499-511.

RUTA, V., DATTA, S. R., VASCONCELOS, M. L., FREELAND, J., LOOGER, L. L. & AXEL, R. 2010. A dimorphic pheromone circuit in Drosophila from sensory input to descending output. *Nature,* 468**,** 686-90.

SACHSE, S. & GALIZIA, C. G. 2003. The coding of odour-intensity in the honeybee antennal lobe: local computation optimizes odour representation. *Eur J Neurosci,* 18**,** 2119-32.

SAKURAI, T., NAMIKI, S. & KANZAKI, R. 2014. Molecular and neural mechanisms of sex pheromone reception and processing in the silkmoth Bombyx mori. *Front Physiol,* 5**,** 125.

SATO, K., PELLEGRINO, M., NAKAGAWA, T., NAKAGAWA, T., VOSSHALL, L. B. & TOUHARA, K. 2008. Insect olfactory receptors are heteromeric ligand-gated ion channels. *Nature,* 452**,** 1002-6.

SCHNEIDER, D., SCHULZ, S., PRIESNER, E., ZIESMANN, J. & FRANCKE, W. 1998. Autodetection and chemistry of female and male pheromone in both sexes of the tiger moth Panaxia quadripunctaria. *Journal of Comparative Physiology a-Sensory Neural and Behavioral Physiology,* 182**,** 153-161.

SEKI, Y., AONUMA, H. & KANZAKI, R. 2005. Pheromone processing center in the protocerebrum of Bombyx mori revealed by nitric oxide-induced anti-cGMP immunocytochemistry. *J Comp Neurol,* 481**,** 340-51.

SKIRI, H. T., GALIZIA, C. G. & MUSTAPARTA, H. 2004. Representation of Primary Plant Odorants in the Antennal Lobe of the Moth Heliothis virescens Using Calcium Imaging. *Chemical Senses,* 29**,** 253-267.

STAV, I. V. 2014. *Identification of different antennal-lobe neuron categories;: a morphological and physiological study of second order neurons in the primary olfactory brain centre of the moth Heliothis virescens .* Master's thesis in Biology, Norwegian University of Science and Technology.

STEIN, R. B., GOSSEN, E. R. & JONES, K. E. 2005. Neuronal variability: noise or part of the signal? *Nat Rev Neurosci,* 6**,** 389-97.

STELINSKI, L. L., IL'ICHEV, A. L. & GUT, L. J. 2006. Antennal and behavioral responses of virgin and mated oriental fruit moth (Lepidoptera : Tortricidae) females to their sex pheromone. *Annals of the Entomological Society of America,* 99**,** 898-904.

STRANDEN, M., BORG-KARLSON, A. K. & MUSTAPARTA, H. 2002. Receptor neuron discrimination of the germacrene D enantiomers in the moth Helicoverpa armigera. *Chem Senses,* 27**,** 143-52.

STRAUSFELD, N. J. 2012. *Arthropod brains : evolution, functional elegance, and historical significance,* Cambridge, Mass., Harvard University Press.

STRAUSFELD, N. J., SINAKEVITCH, I. & OKAMURA, J. Y. 2007. Organization of local interneurons in optic glomeruli of the dipterous visual system and comparisons with the antennal lobes. *Dev Neurobiol,* 67**,** 1267-88.

SUN, X. J., TOLBERT, L. P. & HILDEBRAND, J. G. 1997. Synaptic organization of the uniglomerular projection neurons of the antennal lobe of the moth Manduca sexta: a laser scanning confocal and electron microscopic study. *J Comp Neurol,* 379**,** 2-20.

TANAKA, N. K., AWASAKI, T., SHIMADA, T. & ITO, K. 2004. Integration of chemosensory pathways in the Drosophila second-order olfactory centers. *Curr Biol,* 14**,** 449-57.

TANAKA, N. K., ENDO, K. & ITO, K. 2012. Organization of antennal lobe-associated neurons in adult Drosophila melanogaster brain. *J Comp Neurol,* 520**,** 4067-130.

VALDERHAUG, V. D. 2015. *Morphological characterization of antennal-lobe projection neurons in the olfactory pathway of heliothine moths.* Master's thesis in Neuroscience, Norwegian University of Science and Technology.

WALTERS, E. T., ILLICH, P. A., WEEKS, J. C. & LEWIN, M. R. 2001. Defensive responses of larval Manduca sexta and their sensitization by noxious stimuli in the laboratory and field. *J Exp Biol,* 204**,** 457-69.

WANG, K., GONG, J., WANG, Q., LI, H., CHENG, Q., LIU, Y., ZENG, S. & WANG, Z. 2014. Parallel pathways convey olfactory information with opposite polarities in Drosophila. *Proc Natl Acad Sci U S A,* 111**,** 3164-9.

WEHR, M. & LAURENT, G. 1996. Odour encoding by temporal sequences of firing in oscillating neural assemblies. *Nature,* 384**,** 162-6.

WEISSLING, T. J. & KNIGHT, A. L. 1996. Oviposition and calling behavior of codling moth (Lepidoptera: Tortricidae) in the presence of codlemone. *Annals of the Entomological Society of America,* 89**,** 142-147.

ZHAO, X. C., CHEN, Q. Y., GUO, P., XIE, G. Y., TANG, Q. B., GUO, X. R. & BERG, B. G. 2016. Glomerular Identification in the Antennal Lobe of the Male Moth, Helicoverpa armigera. *J Comp Neurol*.

ZHAO, X. C., KVELLO, P., LOFALDLI, B. B., LILLEVOLL, S. C., MUSTAPARTA, H. & BERG, B. G. 2014. Representation of pheromones, interspecific signals, and plant odors in higher olfactory centers; mapping physiologically identified antennal-lobe projection neurons in the male heliothine moth. *Front Syst Neurosci,* 8**,** 1-14.

ZHAO, X. C., PFUHL, G., SURLYKKE, A., TRO, J. & BERG, B. G. 2013. A multisensory centrifugal neuron in the olfactory pathway of heliothine moths. *J Comp Neurol,* 521**,** 152-68.

Appendix

The appendix includes figures not shown in the results.

A1 | Morphology and physiology of the antennal lobe interneuron

A2 | Morphology of the protocerebral-calycal tract

A3 | Trial to trial maximum firing rate

A4 | Trial to trial response duration

A1 | **Morphology and physiology of the antennal lobe interneuron**

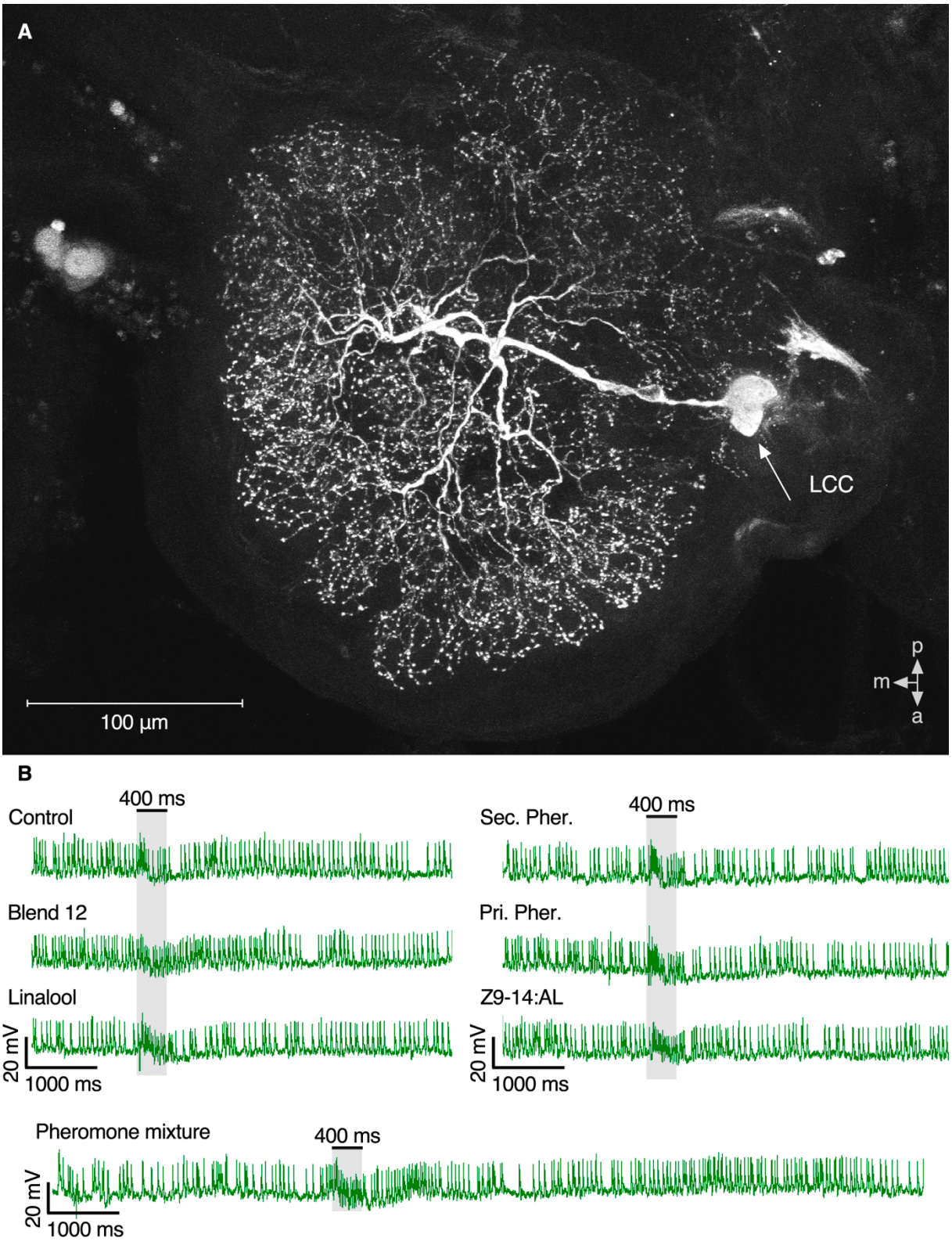

Figure A1 | **Antennal lobe interneuron**. An accidentally stained antennal lobe (AL) interneuron was seen in confocal images of a 7 days old male *H. armigera*. **A)** The AL interneuron is shown by confocal imaging. Stain and recording is most likely done in the somata located in the lateral cell cluster (LCC). **B)** The interneuron showed a broad, but modest response pattern, most responsive to the ideal pheromone mixture as well as the primary and secondary pheromone component alone.

A2 | **Morphology of the protocerebral-calycal tract**

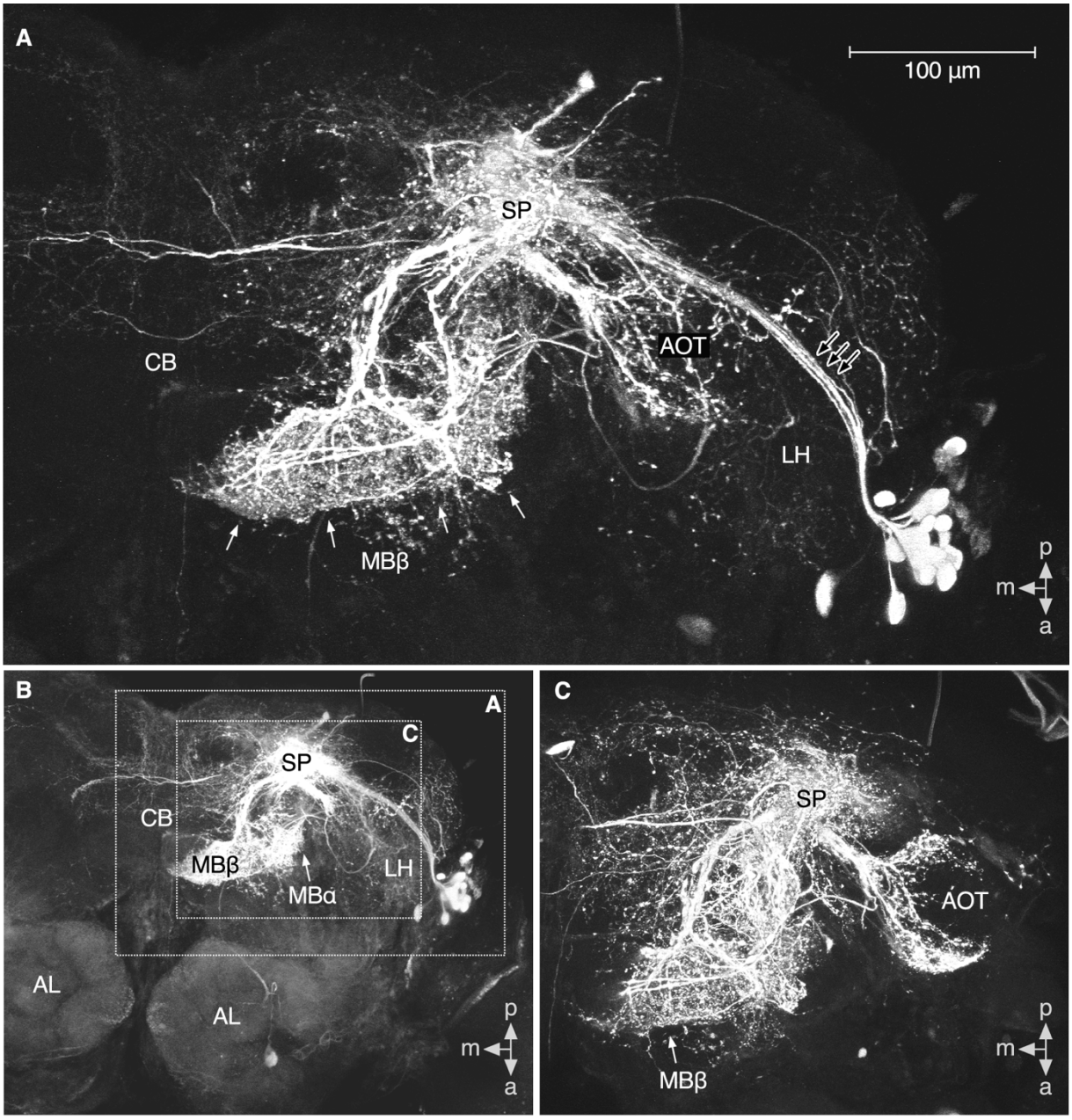

Figure A2 | **The protocerebral-calycal tract.** One stained preparation, a 2 days old male *H. virescens,* showed staining of several neurons. **A)** Confocal image displaying the protocerebral-calycal tract (PCT). In total 14 stained cell bodies could be counted, all clustered in the lateral protocerebrum. The tract projects toward the superior protocerebrum (SP), where branches innervate both the mushroom body peduncle and calyx, before the projections turn to innervate parts of the alpha lobe of the mushroom body (MBα) and parts of the mushroom body beta lobe (MBβ). Four white arrows indicate the MBβ. Three black arrows indicate the PCT. **B)** Confocal image indicating the overall position of the magnified pictures shown in A and C. **C)** This figure shows a stack of confocal images obtained more dorsally in the preparation than those in A. Here, innervations in the outer part of the anterior optic tubercle (AOT) could be seen. These innervations seemed to originate from two to three neurons, which cell bodies most likely were confined to the same cell body cluster as the protocerebral-calycal tract neurons. White arrow points toward the MBβ. *a = Anterior; AL = Antennal lobe; CB = Central body; LH = Lateral horn; m = Medial; p = Posterior.*

A3 | **Trial to trial maximum firing rate**

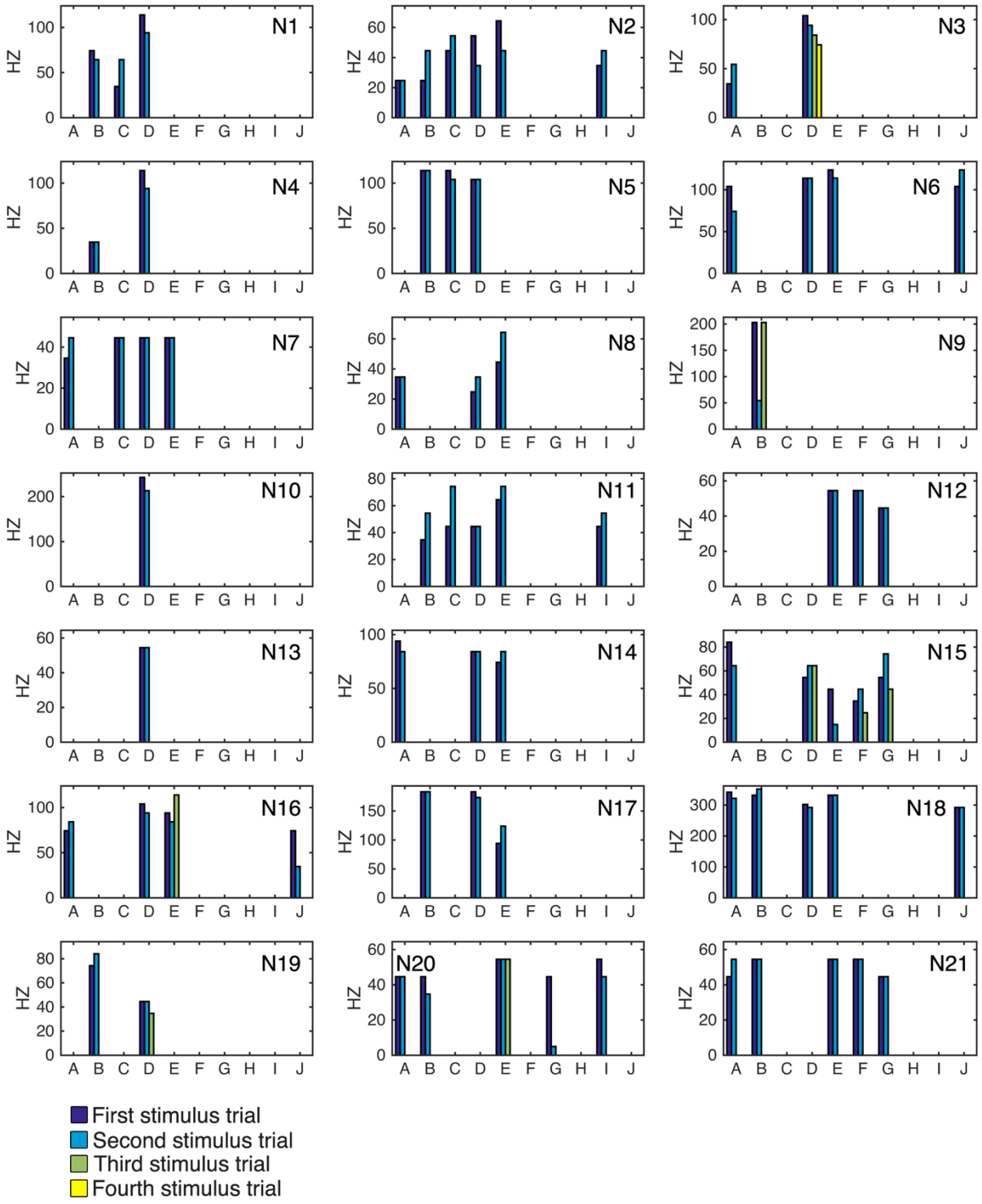

Figure A3 | **Maximum firing rate for each trial**. The maximum firing rate was estimated for each stimulus trial in a 2500 ms time window after stimulus onset. The histograms show the max firing rate for consecutive trials of odorants that were found to show a significant response. A = Control (hexane); B = Blend 12; C = linalool; D = Sunflower; E = Pheromone mixture; F = Primary pheromone component; G = Secondary pheromone component; H = Germacrene D; I = Interspecific signal 1; J = Interspecific signal 2.

A4 | **Trial to trial response duration**

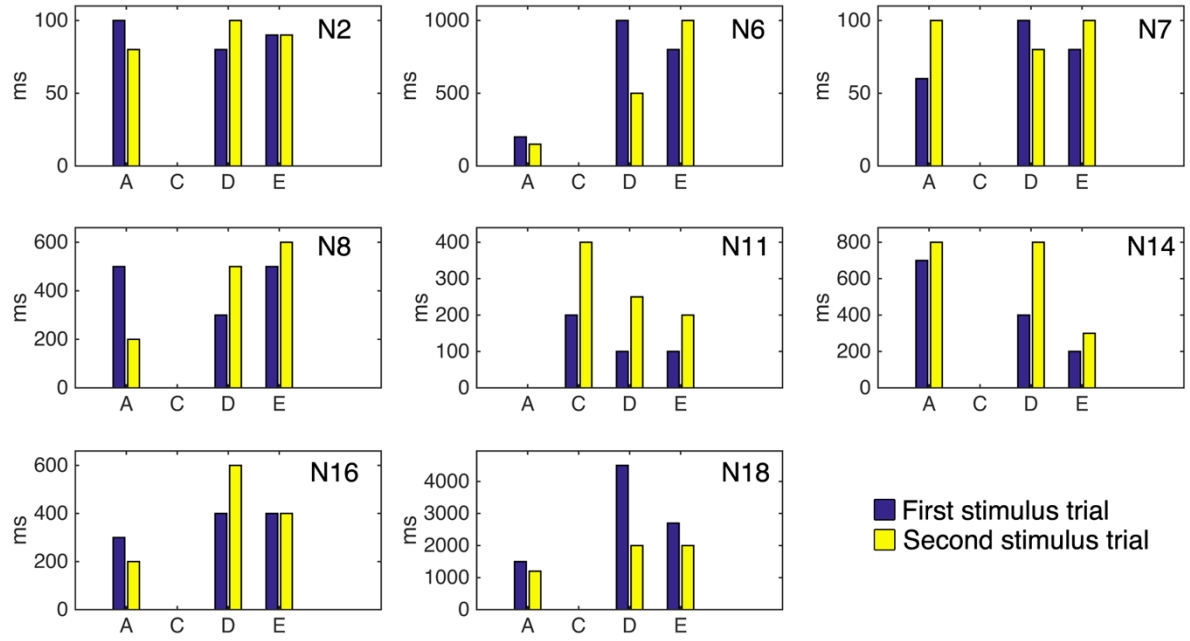

Figure A4 | **Response duration for each stimulus trial**. Each histogram shows the response duration of 4 substances which was subjectively estimated by examining the spike train data. The histograms display the response duration for the first and second stimulus trial for each tested substance. Clear differences in response duration for consecutive trials can be seen in both N6, N8, N11, N14 and N18. A = Control (hexane); C = Linalool; D = Sunflower; E = Ideal pheromone mixture.